Supporting Information

Synthesis and Photophysical Properties of Europium(III)-*β*-Diketonate Complexes Applied in LED

Guang Shao[*a], Huijuan Yu[a], Na Zhang[a], Yanjian He, Kejun Feng[b], Xin Yang[c], Rihui Cao[*a], Menglian Gong[a]

[a] School of Chemistry and Chemical Engineering, Sun Yat-sen University, Guangzhou, 510275, PR China

[b] Department of Chemical Engineering, Hui-Zhou University, Huizhou 516007, PR China

[c] Department of Chemistry and Center for Photochemical Sciences, Bowling Green State University, Bowling Green, Ohio 43403, United States

---

*Corresponding authors. Tel/Fax: +86-20-84110918. E-mail addresses: shaog@mail.sysu.edu.cn (G. Shao); caorihui@mail.sysu.edu.cn (R. Cao)

Contents:

1. Synthesis of compounds **1c**–**f**, ligands **2c**–**e**, complexes **3c**–**e** and gadolinium(III) binary complexes
2. FT-IR spectra of ligands **2c**–**f** and complexes **3c**–**f**
3. ^{1}H NMR spectra of compounds **1c**–**f**; ^{1}H, ^{13}C NMR, ^{19}F NMR and EI-MS spectra of ligands **2c**–**f**; ^{1}H and ^{19}F NMR spectra of complexes **3c**–**f**
4. TGA and DTG of complexes **3a**–**f**
5. Magnified emission spectra of complexes **3a**–**f**
6. $^5D_0$ decay profiles of complexes **3a**–**f**
7. Phosphorescence spectra of gadolinium(III) binary complexes
8. CV curves of ligands **2a**–**f**
9. Emission spectra and photographs of the fabricated LEDs
10. CIE chromaticity coordinates based on the emission spectra of the fabricated LEDs

1. Synthesis of compounds 1c–f, ligands 2c–e, complexes 3c–e and gadolinium(III) binary complexes

Compound 1c

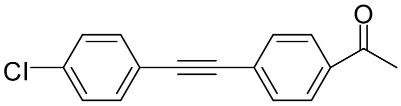

A 100 mL flask was charged with 4-chlorophenylacetylene (1.50 g, 11.00 mmol), 4-iodoacetophenone (2.46 g, 10.00 mmol), $Pd(PPh_3)_4$ (346 mg, 0.30 mmol), CuI (95 mg, 0.50mmol), diisopropylamine (10 mL) and toluene (60 mL). After being stirred under argon at 60 °C for 12 h, the reaction mixture was cooled to room temperature and filtered. The filtrate was poured into aqueous NH_4Cl and extracted with ethyl acetate. The extract was then washed with brine, dried over magnesium sulfate and filtered. After evaporation at a reduced pressure, the residue was subjected to column chromatography on silica gel (hexane/ethyl acetate = 10/1), affording the product as solids (2.29 g, 90.0 %). ^{1}H NMR (300 MHz, $CDCl_3$): δ (ppm) 2.61(s, 3H), 7.32(d, J = 8.4 Hz, 2H), 7.45(d, J = 8.4 Hz, 2H), 7.57(d, J = 8.1 Hz, 2H), 7.92(d, J = 8.1 Hz, 2H).

Compound 1d

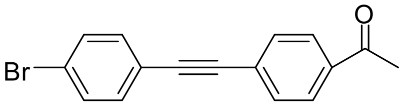

A 100 mL flask was charged with 4-bromophenylacetylene (1.16 g, 6.43 mmol), 4-iodoacetophenone (1.74 g, 7.07 mmol), $Pd(PPh_3)_4$ (220 mg, 0.19 mmol), CuI (59 mg, 0.31 mmol), diisopropylamine (5 mL) and toluene (40 mL). After being stirred under argon at 50 °C for 12 h, the reaction mixture was cooled to room temperature and filtered. The filtrate was poured into aqueous NH_4Cl and extracted with ethyl acetate. The extract was then washed with brine, dried over magnesium sulfate and filtered. After evaporation at a reduced pressure, the residue was subjected to column chromatography on silica gel (hexane/ethyl acetate = 20/1), affording the product as solids (1.69 g, 88.0 %). ^{1}H NMR (300 MHz, $CDCl_3$): δ (ppm) 2.61(s, 3H), 7.38(d, J = 8.4 Hz, 2H), 7.48(d, J = 8.4 Hz, 2H), 7.57(d, J = 8.1 Hz, 2H), 7.92(d, J = 8.4 Hz, 2H).

Compound 1e

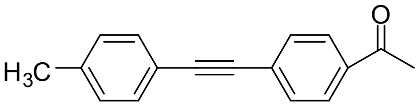

A 50 mL flask was charged with 4-ethynyltoluene (697 mg, 6.00 mmol), 4-iodoacetophenone (1.23 g, 5.00 mmol), $Pd(PPh_3)_4$ (173 mg, 0.15 mmol), CuI (48 mg, 0.25 mmol), diisopropylamine (5 mL) and toluene (40 mL). After being stirred under argon at 60 °C for 12 h, the reaction mixture was cooled to room temperature and filtered. The filtrate was poured into aqueous NH_4Cl and extracted with ethyl acetate. The extract was then washed with brine, dried over magnesium sulfate and filtered. After evaporation at a reduced pressure, the residue was subjected to column chromatography on silica gel (hexane/ethyl acetate = 10/1), affording the product as solids (1.02 g, 87.0 %). ^{1}H NMR (300 MHz, $CDCl_3$): δ (ppm) 2.37(s, 3H), 2.61(s, 3H), 7.16(d, J = 7.8 Hz, 2H), 7.42(d, J = 7.8 Hz, 2H), 7.57(d, J = 7.8 Hz, 2H), 7.91(d, J = 7.8 Hz, 2H).

Compound 1f

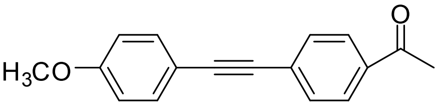

A 25 mL flask was charged with 4-ethynylanisole (132 mg, 1.00 mmol), 4-iodoacetophenone (295 mg, 1.20 mmol), $Pd(PPh_3)_4$ (58 mg, 0.05 mmol), CuI (10 mg, 0.05 mmol), diisopropylamine (1 mL) and toluene (10 mL). After being stirred under argon at 50 °C for 12 h, the reaction mixture was cooled to room temperature and filtered. The filtrate was poured into aqueous NH_4Cl and extracted with ethyl acetate. The extract was then washed with brine, dried over magnesium sulfate and filtered. After evaporation at a reduced pressure, the residue was subjected to column chromatography on silica gel (hexane/ethyl acetate = 20/1), affording the product as solids (211 mg, 84.7 %). ^{1}H NMR (300 MHz, $CDCl_3$): δ (ppm) 2.60(s, 3H), 3.82(s, 3H), 6.87(d, J = 8.7 Hz, 2H), 7.46(d, J = 9.0 Hz, 2H), 7.55(d, J = 8.7 Hz, 2H), 7.90(d, J = 8.1 Hz, 2H).

Ligand 2c

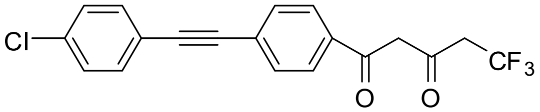

A 50 mL flask was charged with compound **1c** (1.79 g, 7.06 mmol), sodium hydride (848 mg, 35.33 mmol) and toluene (25 mL). After being stirred under argon at 0 °C for 1 h, ethyl trifluoroacetate (3.01 g, 21.20 mmol) was added dropwise at 0 °C. The reaction was warmed up and stirred at 30 °C for 12 hour. After reaction, H_2O (25 mL) was added to quench the reaction. The pH value of aqueous phase was adjusted to 4.0-5.0 with hydrochloric acid (1.0 mol/L). The reaction mixture was extracted with ethyl acetate. The extract was then dried over magnesium sulfate and filtered. After evaporation at a reduced pressure, the residue was subjected to column chromatography on silica gel (hexane), affording the product as solids (1.66 g, 67.0 %). ^{1}H NMR (300 MHz, $CDCl_3$): δ (ppm) 6.55(s, 1H), 7.33(d, J = 7.6 Hz, 2H), 7.46(d, J = 7.6 Hz, 2H), 7.60(d, J = 6.7 Hz, 2H), 7.90(d, J = 6.7 Hz, 2H). ^{13}C NMR (75 MHz, $CDCl_3$): δ (ppm) 89.26, 92.29, 92.47, 116.96(CF_3, q, J_{C-F} = 281.3 Hz), 120.79, 127.38, 128.70, 128.74, 131.82, 131.97, 132.82, 134.98, 177.44(C-CF_3, q, J_{C-F} = 35.7 Hz), 184.39. ^{19}F NMR (282 MHz, $CDCl_3$): δ (ppm) -77.12. FT-IR (KBr) v_{max}(cm^{-1}): 3432, 3135, 3058, 2850, 2214, 1601, 1506, 1485, 1317, 1296, 1253, 1197, 1150, 1127, 1105, 1092, 1011, 917, 855, 827, 802, 741, 688, 620, 582, 514. MS (EI) *m/z* (%): 352 (31) [M^++2], 351 (19) [M^++1], 350 (100) [M^+], 281 (68) [M^+-69], 239 (55) [M^+-111], 69 (22) [M^+-281].

Ligand 2d

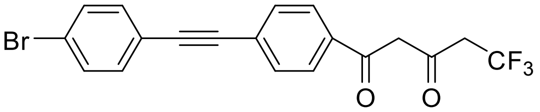

A 25 mL flask was charged with compound **1d** (341 mg, 1.14 mmol), sodium hydride (137 mg, 5.70 mmol) and toluene (10 mL). After being stirred under argon at 0 °C for 1 h, ethyl trifluoroacetate (486 mg, 3.42 mmol) was added dropwise at 0 °C. The reaction was warmed up and stirred at 30 °C for 12 hour. After reaction, H_2O (10 mL) was added to quench the reaction. The pH value of aqueous phase was adjusted to 4.0-5.0 with hydrochloric acid (1.0 mol/L). The reaction mixture was extracted with ethyl acetate. The extract was then dried over magnesium sulfate and filtered. After evaporation at a reduced pressure, the residue was subjected to column chromatography on silica gel (hexane), affording the product as solids (340 mg, 75.5 %). ^{1}H NMR (300 MHz, $CDCl_3$): δ (ppm) 6.56(s, 1H), 7.39(d, *J* = 8.4 Hz, 2H), 7.49(d, *J* = 8.1 Hz, 2H), 7.61(d, *J* = 8.1 Hz, 2H), 7.92(d, *J* = 8.4 Hz, 2H). ^{13}C NMR (75 MHz, $CDCl_3$): δ (ppm) 89.43, 92.34, 92.53, 116.96(CF_3, q, $J_{C\text{-}F}$ = 281.3 Hz), 121.26, 123.29, 127.42, 128.74, 131.65, 131.86, 132.04, 133.02, 177.50(C-CF_3, q, $J_{C\text{-}F}$ = 36.0 Hz), 184.41. ^{19}F NMR (282 MHz, $CDCl_3$): δ (ppm) -77.19. FT-IR (KBr) ν_{max}(cm^{-1}): 3400, 2923, 2210, 1597, 1480, 1321, 1288, 1199, 1146, 1103, 1065, 1007, 910, 825, 798, 733, 680, 579, 508. MS (EI) *m/z* (%): 396 (43) [M^++1], 394 (43) [M^+-1], 327 (39) [M^++1-69], 325 (39) [M^+-1-69], 285 (19) [M^++1-111], 283 (19) [M^+-1-111], 69 (100) [M^+-326].

Ligand 2e

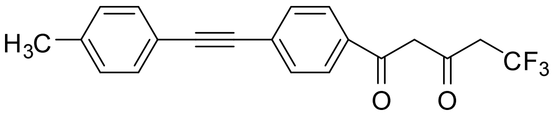

A 50 mL flask was charged with compound **1e** (703 mg, 3.00 mmol), sodium hydride (432 mg, 18.00 mmol) and toluene (25 mL). After being stirred under argon at 0 °C for 1 h, ethyl trifluoroacetate (1.28 g, 9.00 mmol) was added dropwise at 0 °C. The reaction was warmed up and stirred at 30 °C for 12 h. After reaction, H_2O (25 mL) was added to quench the reaction. The pH value of aqueous phase was adjusted to 4.0-5.0 with hydrochloric acid (1.0 mol/L). The reaction mixture was extracted with ethyl acetate. The extract was then dried over magnesium sulfate and filtered. After evaporation at a reduced pressure, the residue was subjected to column chromatography on silica gel (hexane), affording the product as solids (713 mg, 72.0 %). ^{1}H NMR (600 MHz, $CDCl_3$): δ (ppm) 2.36(s, 3H), 6.53(s, 1H), 7.15(d, *J* = 7.8 Hz, 2H), 7.42(d, *J* = 8.4 Hz, 2H), 7.58(d, *J* = 8.4 Hz, 2H), 7.87(d, *J* = 9.0 Hz, 2H). ^{13}C NMR (150 MHz, $CDCl_3$): δ (ppm) 21.48, 87.92, 92.25, 94.18, 117.08(CF_3, q, $J_{C\text{-}F}$ = 281.7 Hz), 119.31, 127.46, 129.21, 129.55, 131.67, 131.86, 139.33, 177.50(C-CF_3, q, $J_{C\text{-}F}$ = 36.0 Hz), 184.83. ^{19}F NMR (282 MHz, $CDCl_3$): δ (ppm) -77.11. FT-IR (KBr) ν_{max}(cm^{-1}): 3410, 2923, 2210, 2163, 1625, 1594, 1513, 1448, 1381, 1285, 1254, 1203, 1152, 1105, 1061, 917, 854, 819, 797, 738, 713, 684, 648, 584, 536, 511, 453. MS (EI) *m/z* (%): 330 (94) [M$^+$], 261 (100) [M$^+$-69], 219 (50) [M$^+$-111], 69 (12) [M$^+$-261].

Complex 3c

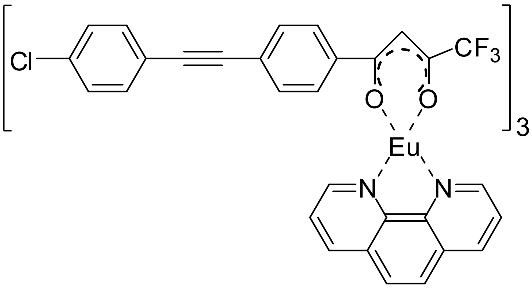

1,10-phenanthroline monohydrate (65 mg, 0.33 mmol) in ethanol (2 mL) was added to a solution of ligand **2c** (350 mg, 1.00 mmol) in ethanol (3 mL) and acetone (2 mL). The resulting mixture was stirred for 5 min at room temperature. To this mixture, europium(III) chloride (85 mg, 0.33 mmol) in EtOH (2 mL) was added dropwise. The pH value of solution was adjusted to 7.0-8.0 with triethylamine. The reaction mixture was stirred at 30 °C for 12 hour. A yellow precipitate appeared and was collected by filtration. The crude product was washed with ethanol and distilled water three times, respectively. After being dried in a high vacuum, 223 mg of product was obtained in 49.0 % yield. ^{1}H NMR (300 MHz, $CDCl_3$): δ (ppm) 3.35(s, 3H), 7.24-7.25(m, 6H), 7.35(d, *J* = 8.1 Hz, 6H), 7.40-7.46(m, 12H), 8.46(d, *J* = 7.8 Hz, 2H), 9.40(bs, 2H), 9.83(s, 2H), 10.40(d, *J* = 7.8 Hz, 2H). Elemental analysis (%): calcd for $C_{66}H_{35}O_6N_2Cl_3F_9Eu$: C, 57.39; H, 2.55; N, 2.03. Found: C, 57.28; H, 2.61; N, 2.04. ^{19}F NMR (282 MHz, $CDCl_3$): δ (ppm) -80.74. FT-IR (KBr) ν_{max}(cm^{-1}): 3435, 2919, 2217, 2136, 1797, 1609, 1549, 1528, 1497, 1306, 1243, 1187, 1140, 1096, 1015, 830, 791, 728, 687, 621, 580.

Complex 3d

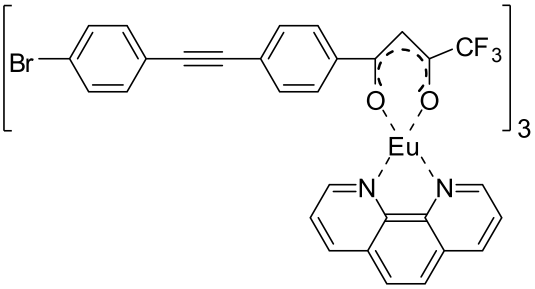

1,10-phenanthroline monohydrate (28 mg, 0.14 mmol) in ethanol (2 mL) was added to a solution of ligand **2d** (170 mg, 0.43 mmol) in ethanol (5 mL) and acetone (1 mL). The resulting mixture was stirred for 5 min at room temperature. To this mixture, europium(III) chloride (36 mg, 0.14 mmol) in EtOH (7 mL) was added dropwise. The pH value of solution was adjusted to 7.0-8.0 with triethylamine. The reaction mixture was stirred at 30 °C for 12 hour. A yellow precipitate appeared and was collected by filtration. The crude product was washed with ethanol and distilled water three times, respectively. After being dried in a high vacuum, 65 mg of product was obtained in 30.6 % yield. ^{1}H NMR (300 MHz, $CDCl_3$): δ (ppm) 3.37(s, 3H), 7.22(d, *J* = 7.5 Hz, 6H), 7.36-7.42(m, 12H), 7.51(d, *J* = 8.4 Hz, 6H), 8.44(d, *J* = 7.8 Hz, 2H), 9.42(bs, 2H), 9.77(s, 2H), 10.36(d, *J* = 7.8 Hz, 2H). Elemental analysis (%): calcd for $C_{66}H_{35}O_6N_2Br_3F_9Eu$: C, 52.34; H, 2.33; N, 1.85. Found: C, 52.26; H, 2.50; N, 1.86. ^{19}F NMR (282 MHz, $CDCl_3$): δ (ppm) -80.80. FT-IR (KBr) ν_{max}(cm^{-1}): 3434, 2215, 1609, 1550, 1529, 1496, 1471, 1429, 1308, 1242, 1186, 1139, 1068, 1010, 944, 850, 827,791, 728, 679, 609, 579, 503, 468.

Complex 3e

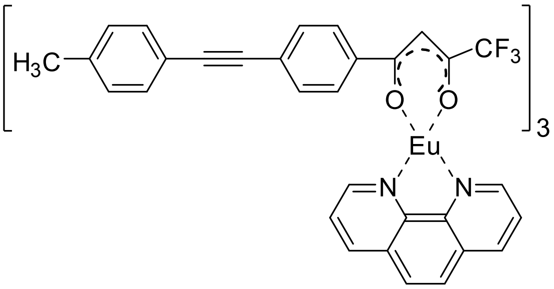

1,10-phenanthroline monohydrate (79 mg, 0.40 mmol) in ethanol (2 mL) was added to a solution of ligand **2e** (396 mg, 1.20 mmol) in a solvent mixture (7 mL of ethanol and 4 mL of acetone). The resulting mixture was stirred for 5 min at room temperature. To this mixture, europium(III) chloride (103 mg, 0.40 mmol) in ethanol (5 mL) was added dropwise. The pH value of solution was adjusted to 7.0-8.0 with triethylamine. The reaction mixture was stirred at 30 °C for 12 h. A yellow precipitate appeared and was collected by filtration. The crude product was washed with ethanol and distilled water three times, respectively. After being dried in a high vacuum, 158 mg of product was obtained in 30.0 % yield. ^{1}H NMR (300 MHz, $CDCl_3$): δ (ppm) 2.41(s, 9H), 3.36(s, 3H), 7.16-7.26(m, 12H), 7.40-7.43(m, 12H), 8.45(d, J = 7.5 Hz, 2H), 9.42(bs, 2H), 9.80(s, 2H), 10.37(d, J = 7.8 Hz, 2H). Elemental analysis (%): calcd for $C_{69}H_{44}O_6N_2F_9Eu$: C, 62.78; H, 3.36; N, 2.12. Found: C, 62.71; H, 3.45; N, 2.21. ^{19}F NMR (282 MHz, $CDCl_3$): δ (ppm) -80.70. FT-IR (KBr) ν_{max}(cm^{-1}): 3439, 2213, 1612, 1550, 1514, 1467, 1426, 1313, 1294, 1243, 1186, 1138, 1108, 1067, 1015, 948, 848, 816, 790, 727, 711, 644, 584, 514.

Gadolinium(III) binary complexes

The synthetic procedures of gadolinium(III) binary complexes have been reported in our earlier publications [1,2]. The elemental analysis data for Gd(**2c**)$_3$·2H_2O ($C_{54}H_{31}Cl_3F_9GdO_8$), Gd(**2d**)$_3$·2H_2O ($C_{54}H_{31}Br_3F_9GdO_8$), Gd(**2e**)$_3$·2H_2O ($C_{57}H_{40}F_9GdO_8$) and Gd(**2f**)$_3$·2H_2O ($C_{57}H_{40}F_9GdO_{11}$) were found (calculated)%: C, 52.01 (52.20), H, 2.39 (2.51); C, 47.42 (47.14), H, 2.65 (2.27); C, 57.48 (57.96), H, 3.09 (3.41) and C, 55.32 (55.70), H, 3.66 (3.28), respectively.

References

(1) G. Shao, N. Zhang, D.A. Lin, K.J. Feng, R.H. Cao, M.L. Gong, A new europium(III)-β-diketonate complex based on diphenylethyne as red phosphors applied in LED, J. Lumin. 138 (2013) 195-200.

(2) H. Wang, P. He, S. Liu, J. Shi, M. Gong, A europium(III) organic ternary complex applied in fabrication of near UV-based white light-emitting diodes, Appl. Phys. B 97 (2009) 481-487.

2. FT-IR spectra of ligands 2c–f and complexes 3c–f

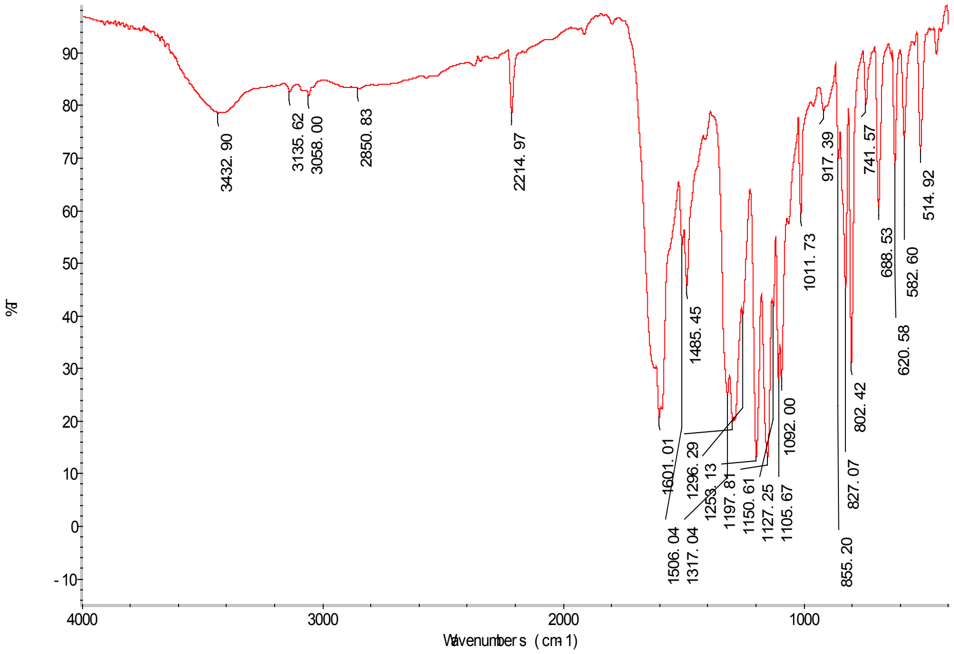

Figure S1. FT-IR (KBr) spectrum of ligand **2c**.

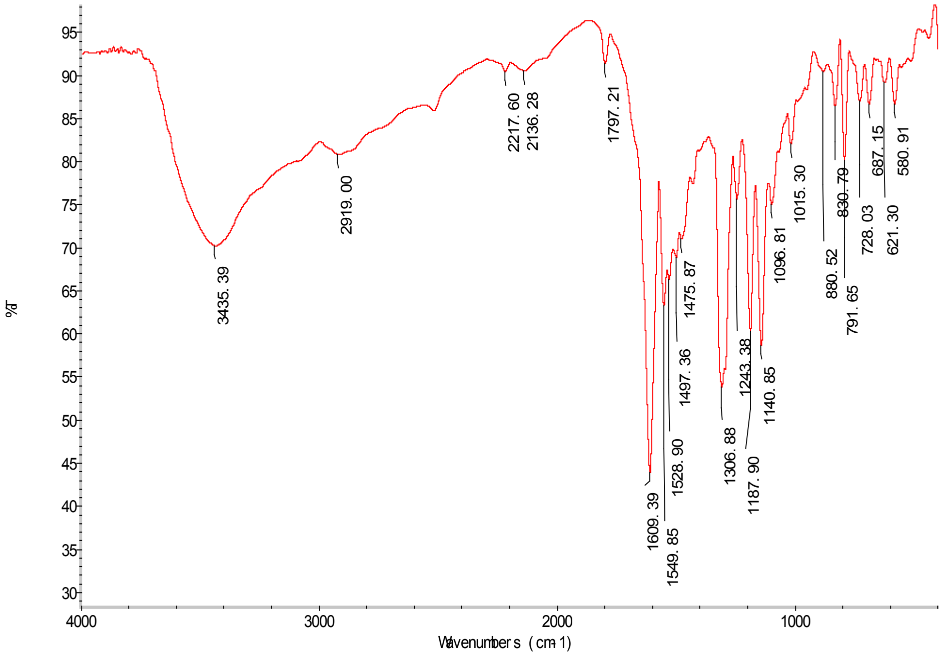

Figure S2. FT-IR (KBr) spectrum of complex **3c**.

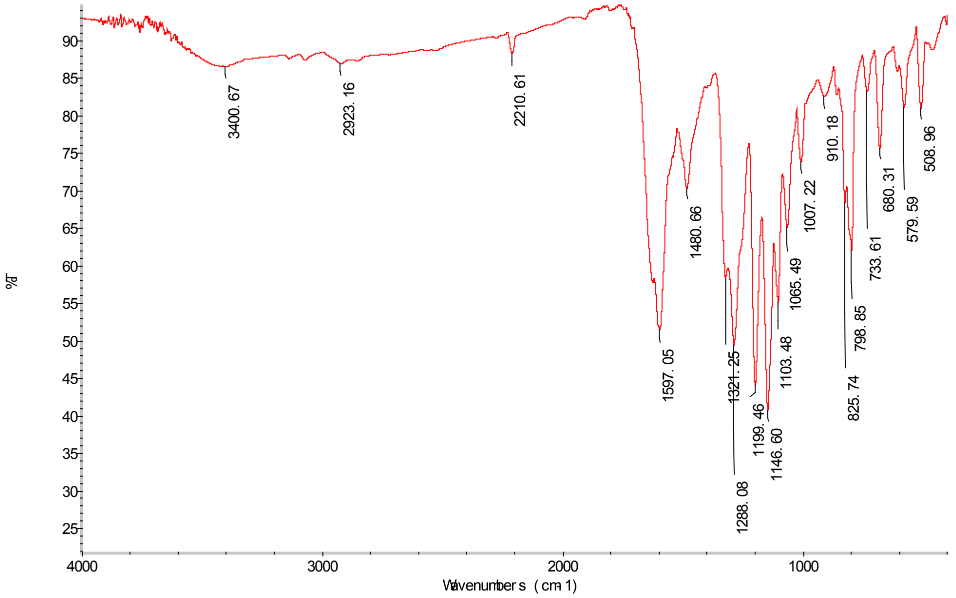

Figure S3. FT-IR (KBr) spectrum of ligand **2d**.

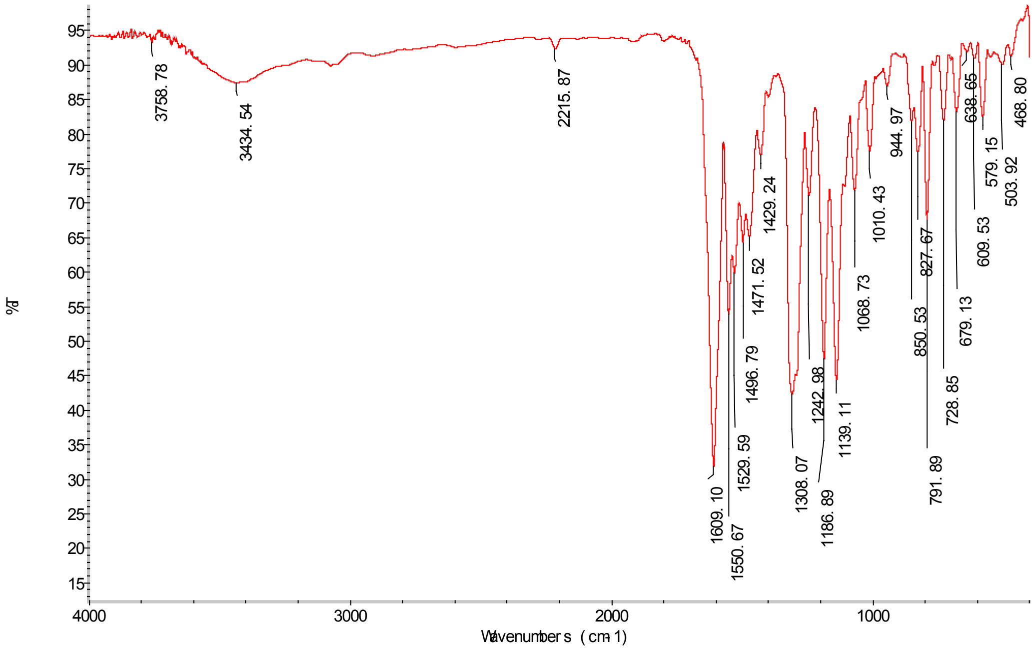

Figure S4. FT-IR (KBr) spectrum of complex **3d**.

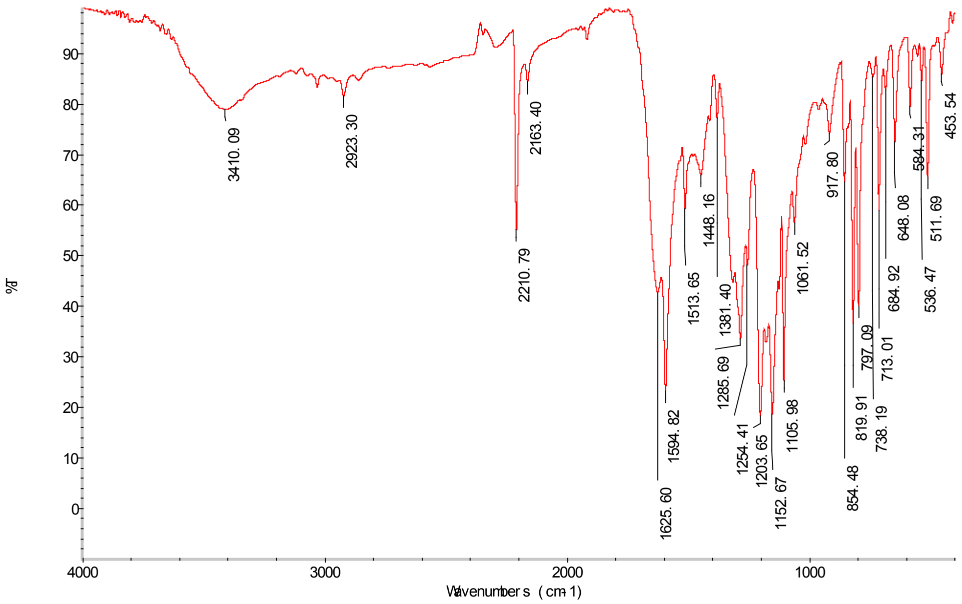

Figure S5. FT-IR (KBr) spectrum of ligand **2e**.

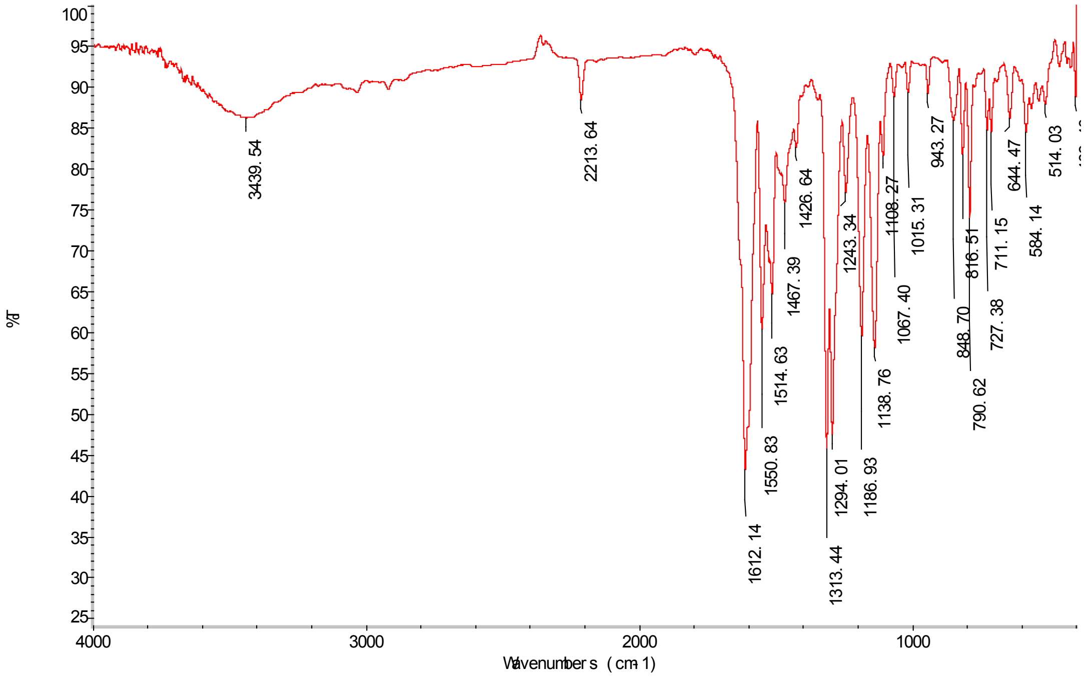

Figure S6. FT-IR (KBr) spectrum of complex **3e**.

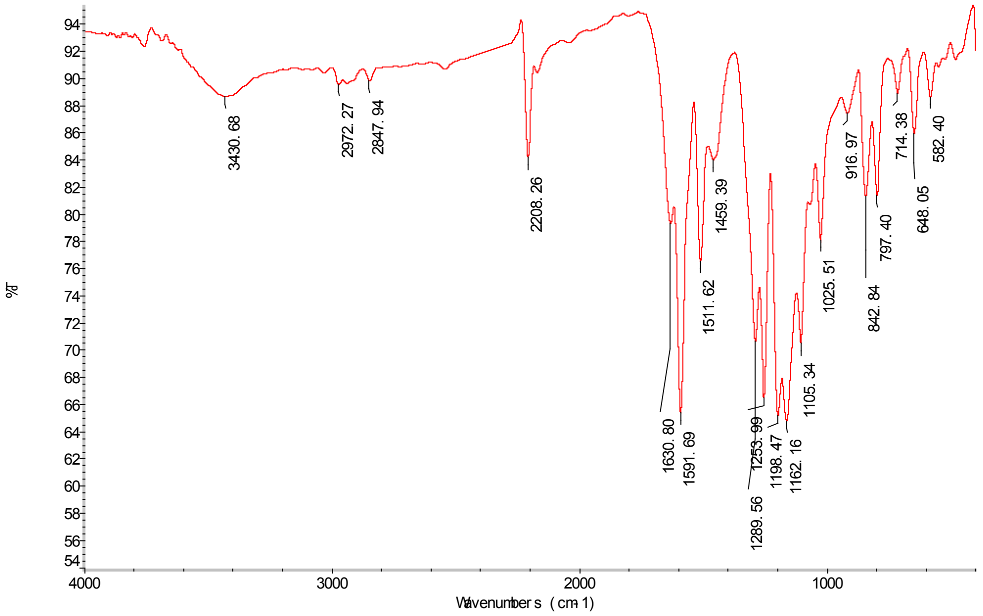

Figure S7. FT-IR (KBr) spectrum of ligand **2f**.

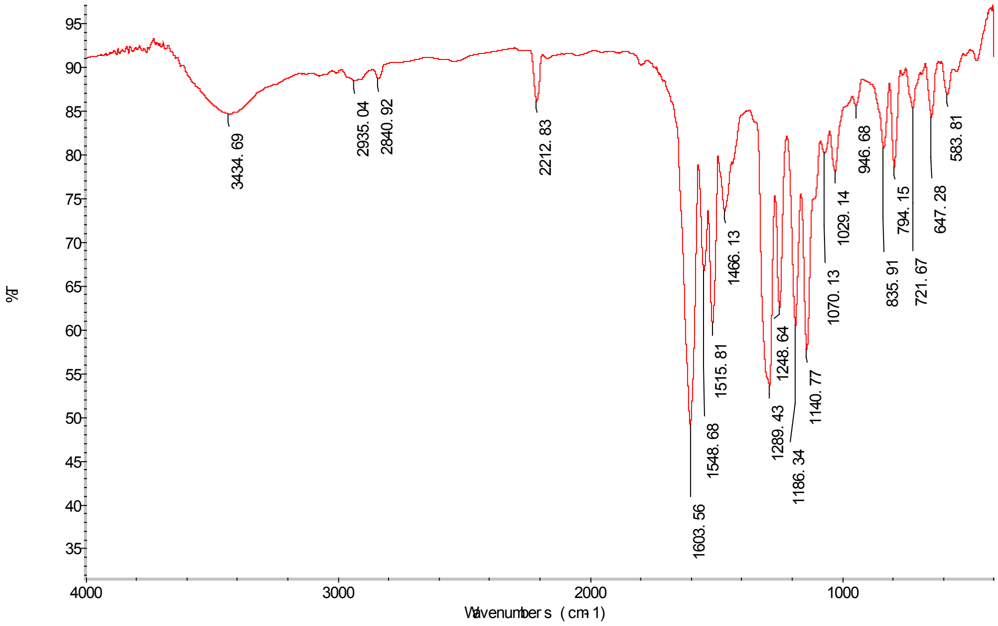

Figure S8. FT-IR (KBr) spectrum of complex **3f**.

3. ^{1}H NMR spectra of compounds 1c–f; ^{1}H, ^{13}C NMR, ^{19}F NMR and EI-MS spectra of ligands 2c–f; ^{1}H and ^{19}F NMR spectra of complexes 3c–f

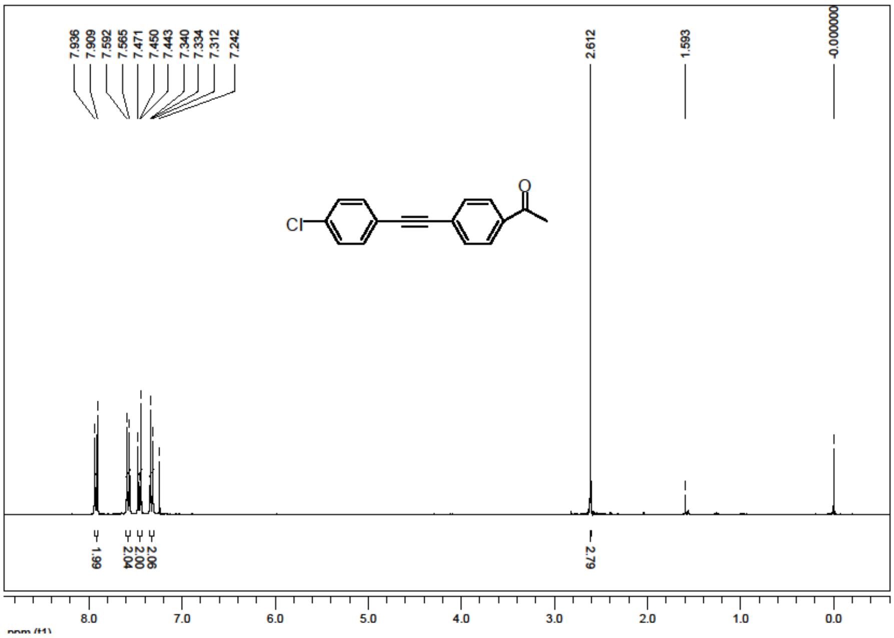

Figure S9. ^{1}H NMR spectrum of compound **1c** (300 MHz, $CDCl_3$).

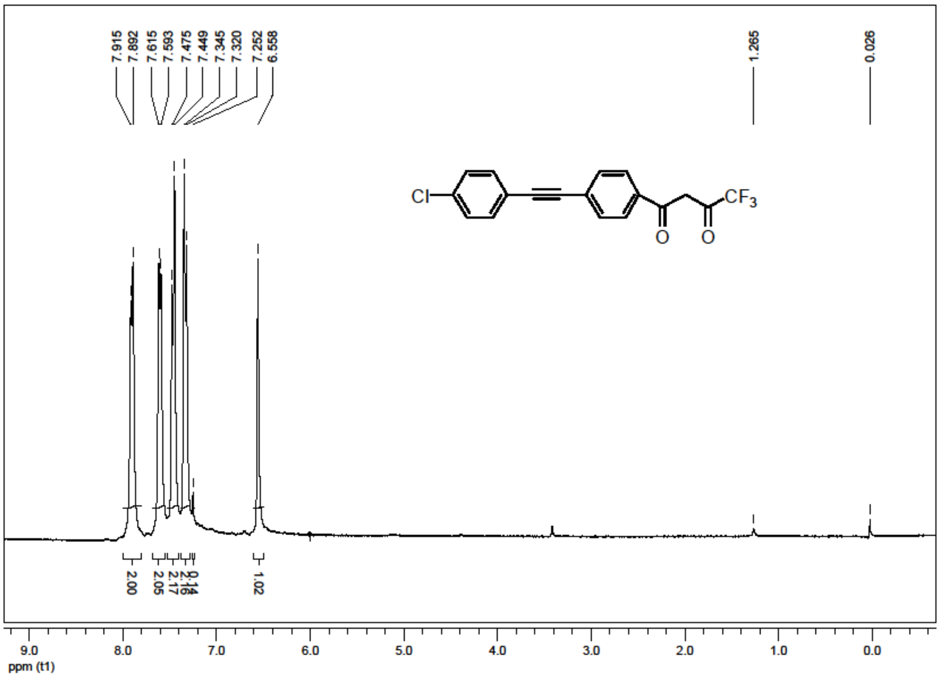

Figure S10. ^{1}H NMR spectrum of ligand **2c** (300 MHz, $CDCl_3$).

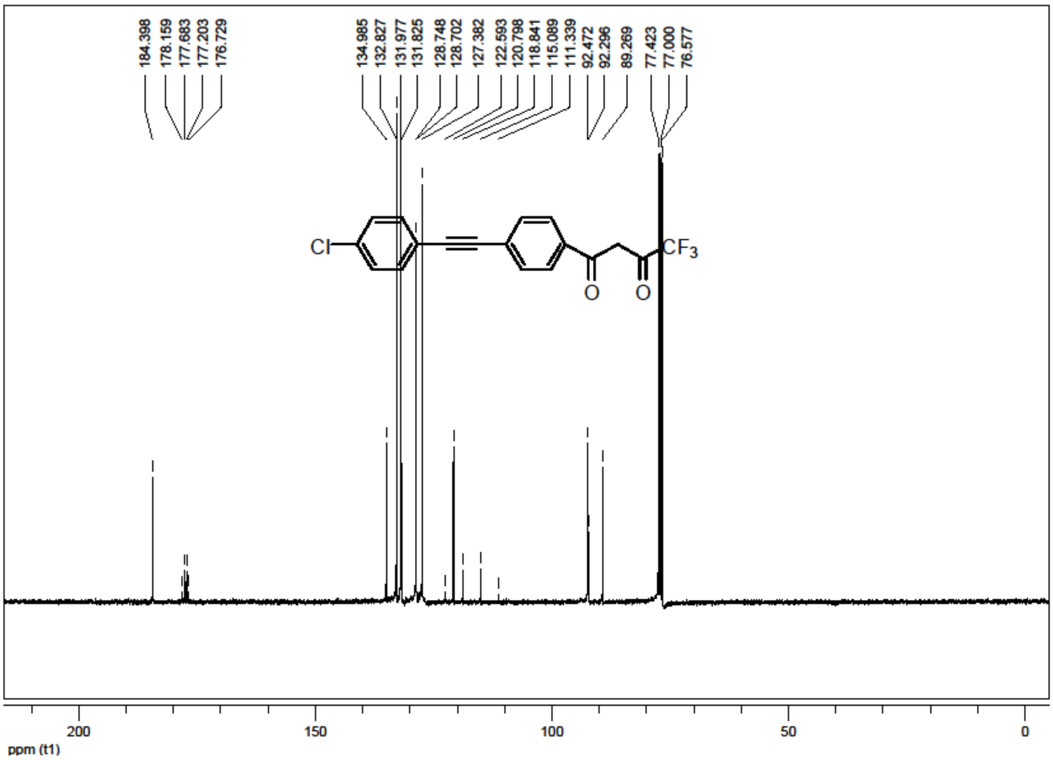

Figure S11. ^{13}C NMR spectrum of ligand **2c** (75 MHz, $CDCl_3$).

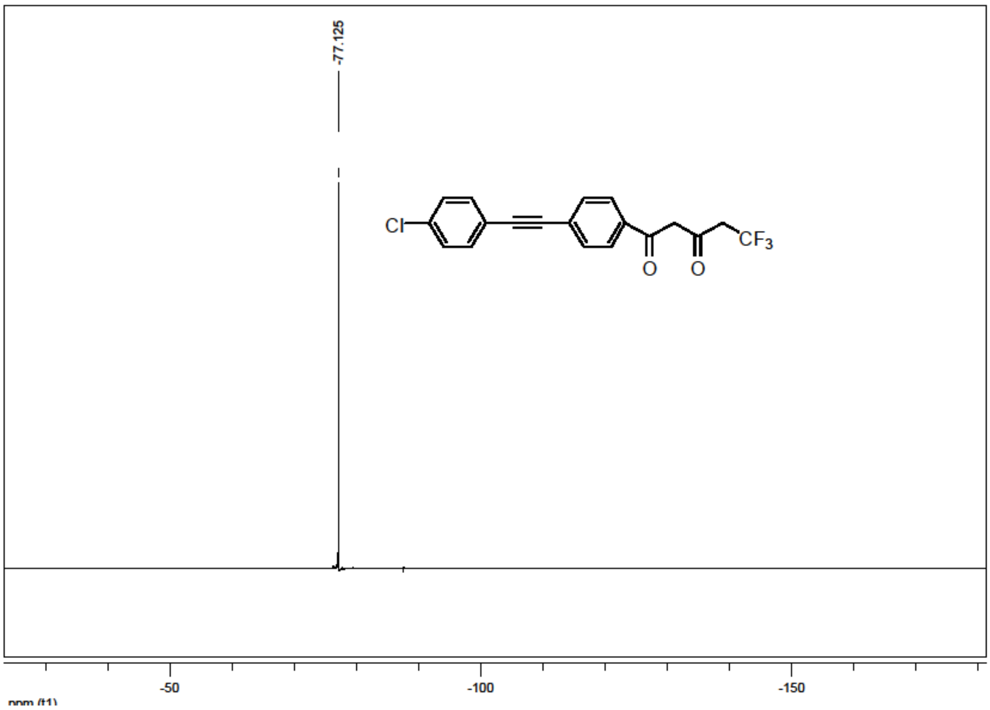

Figure S12. ^{19}F NMR spectrum of ligand **2c** (282 MHz, $CDCl_3$).

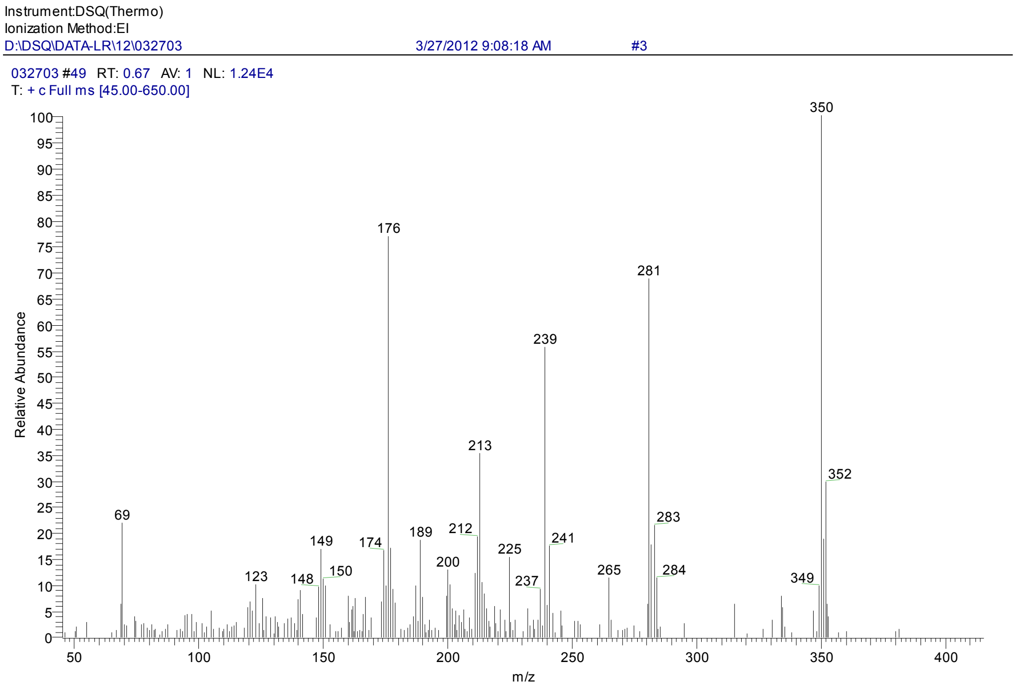

Figure S13. EI-MS spectrum of ligand **2c**.

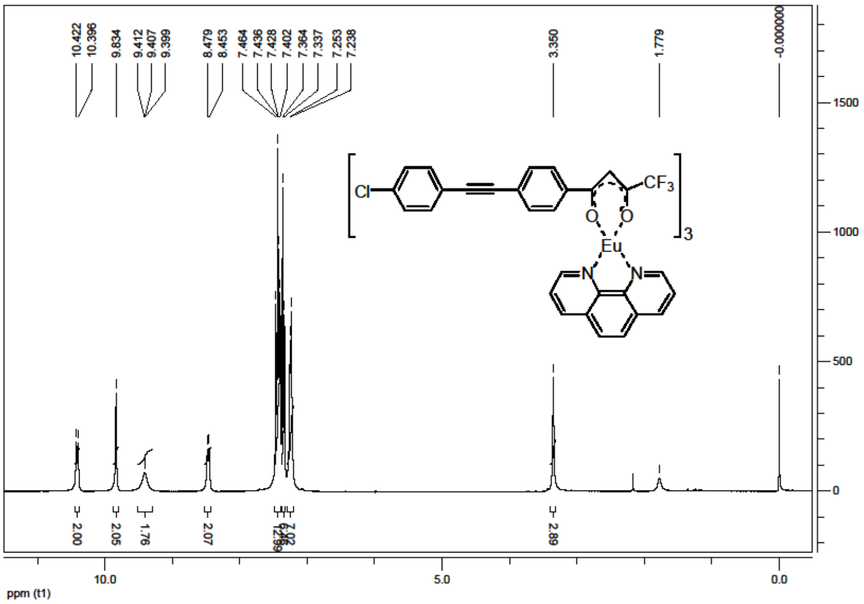

Figure S14. ^{1}H NMR spectrum of complex **3c** (300 MHz, $CDCl_3$).

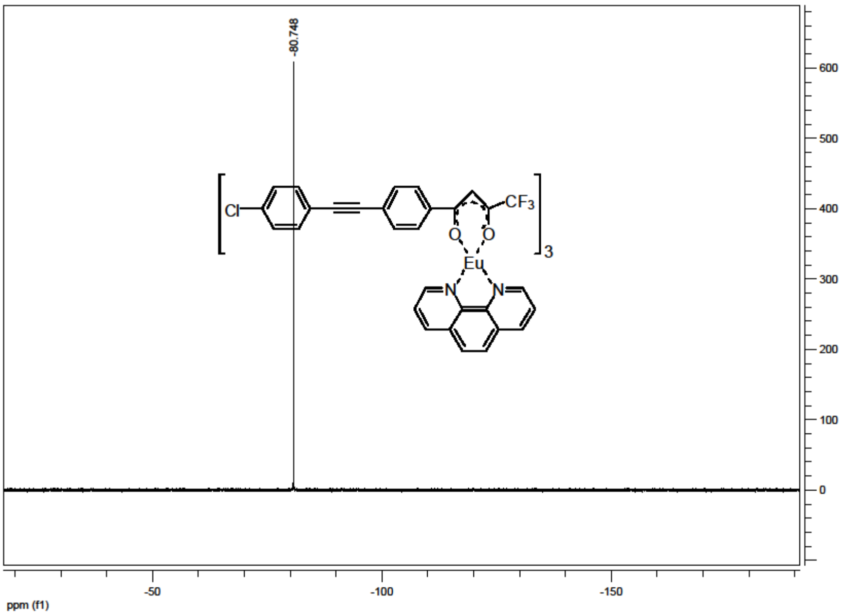

Figure S15. ^{19}F NMR spectrum of complex **3c** (282 MHz, $CDCl_3$).

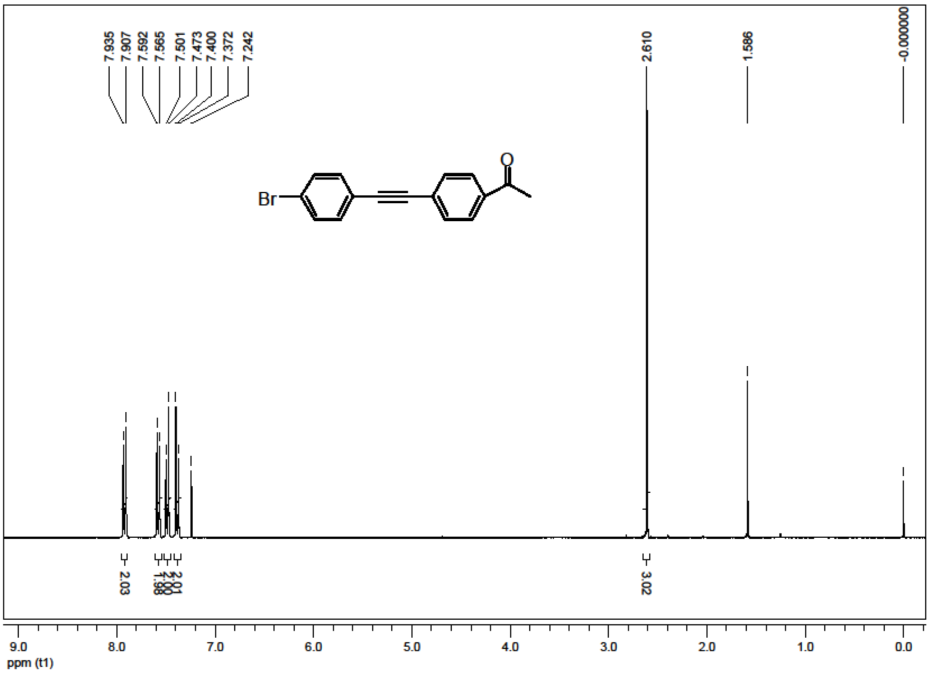

Figure S16. ^{1}H NMR spectrum of compound **1d** (300 MHz, $CDCl_3$).

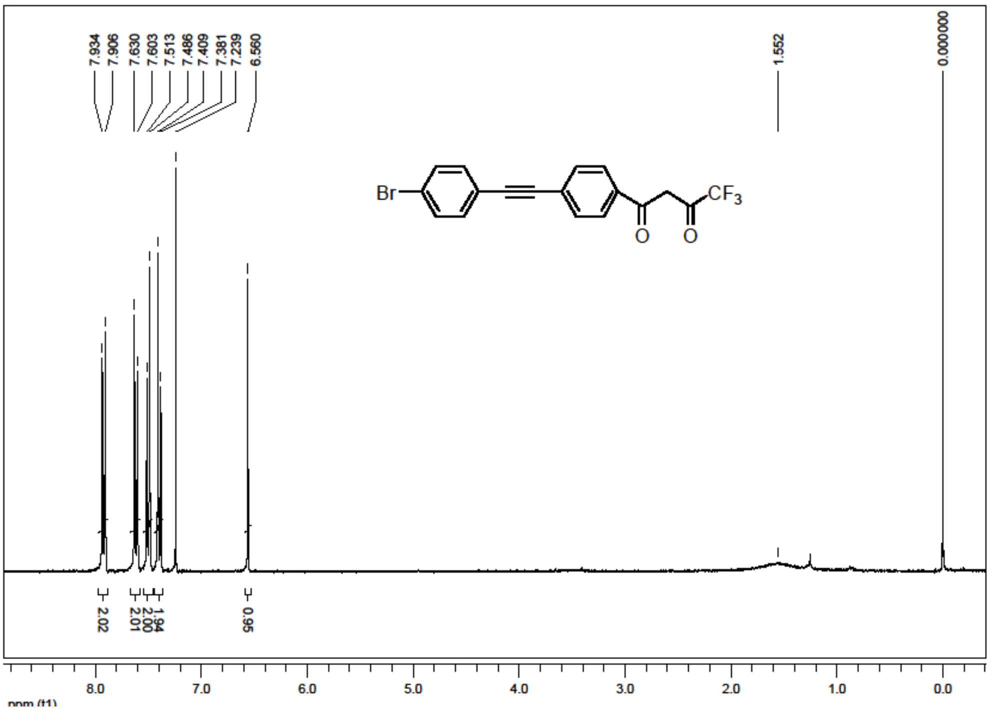

Figure S17. ^{1}H NMR spectrum of ligand **2d** (300 MHz, $CDCl_3$).

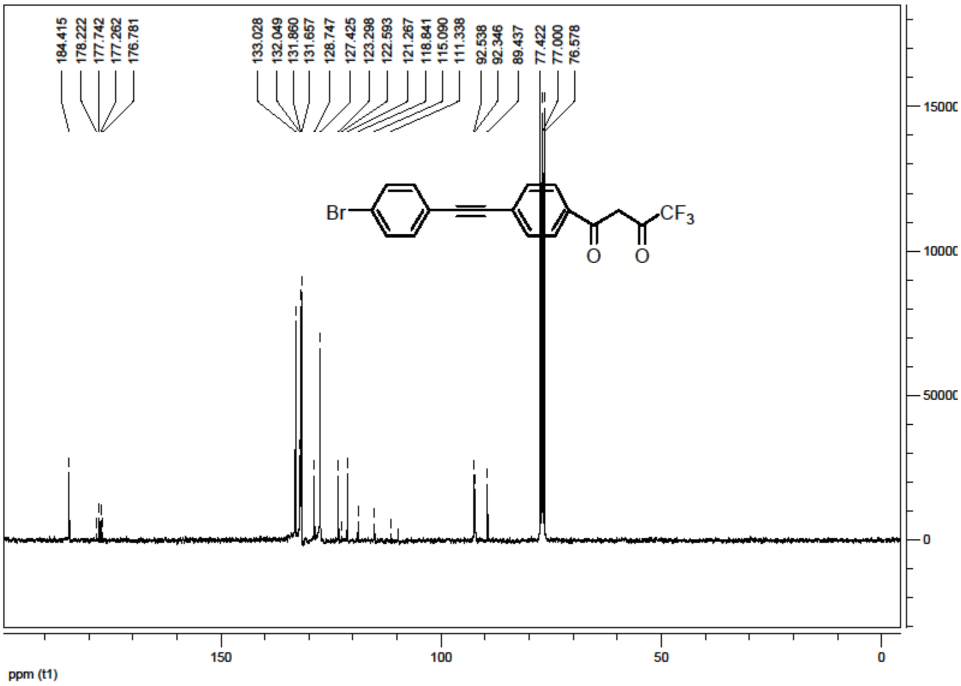

Figure S18. ^{13}C NMR spectrum of ligand **2d** (75 MHz, $CDCl_3$).

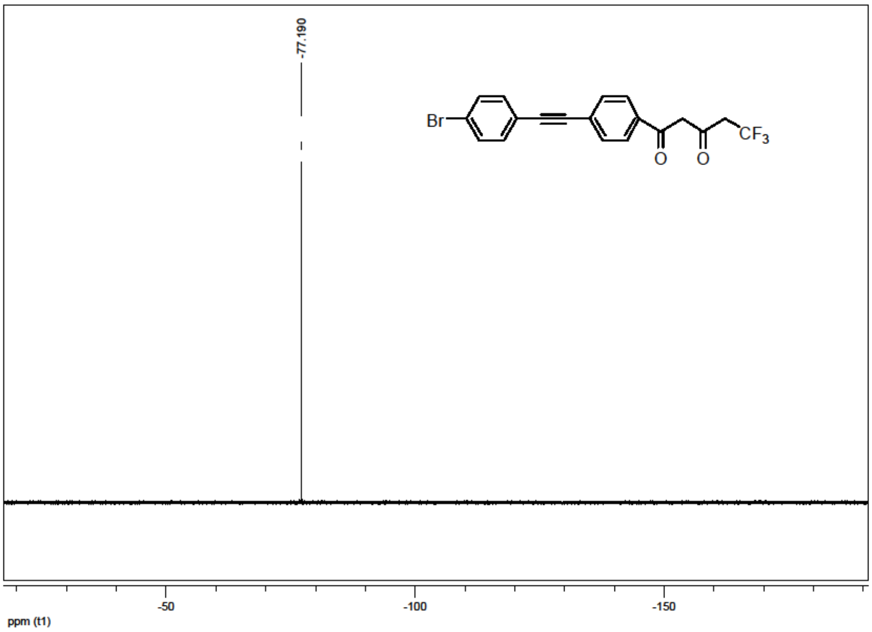

Figure S19. ^{19}F NMR spectrum of ligand **2d** (282 MHz, $CDCl_3$).

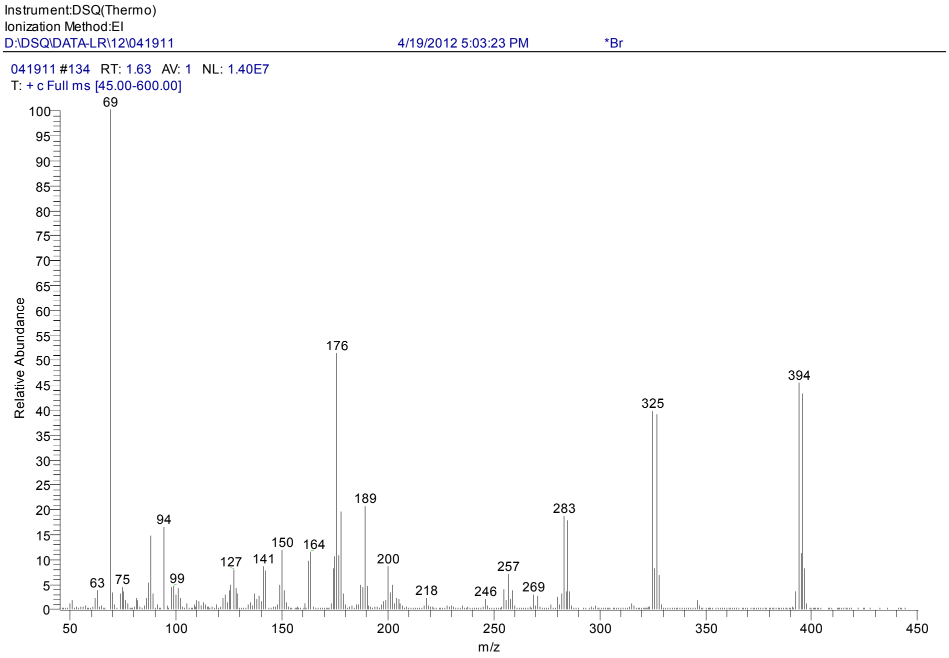

Figure S20. EI-MS spectrum of ligand **2d**.

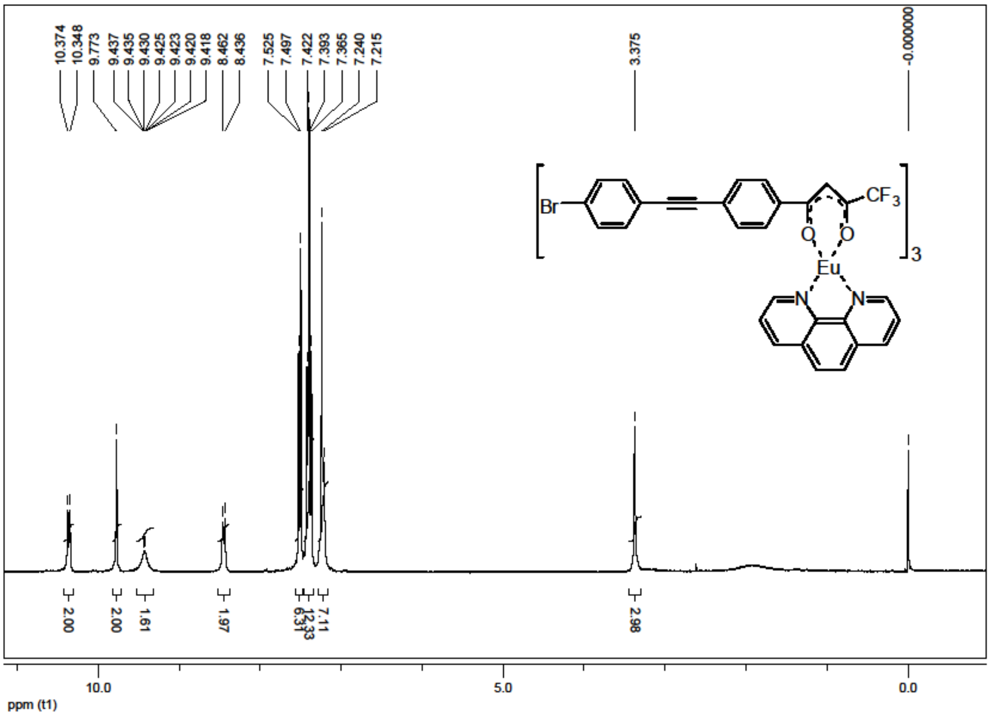

Figure S21. ^{1}H NMR spectrum of complex **3d** (282 MHz, $CDCl_3$).

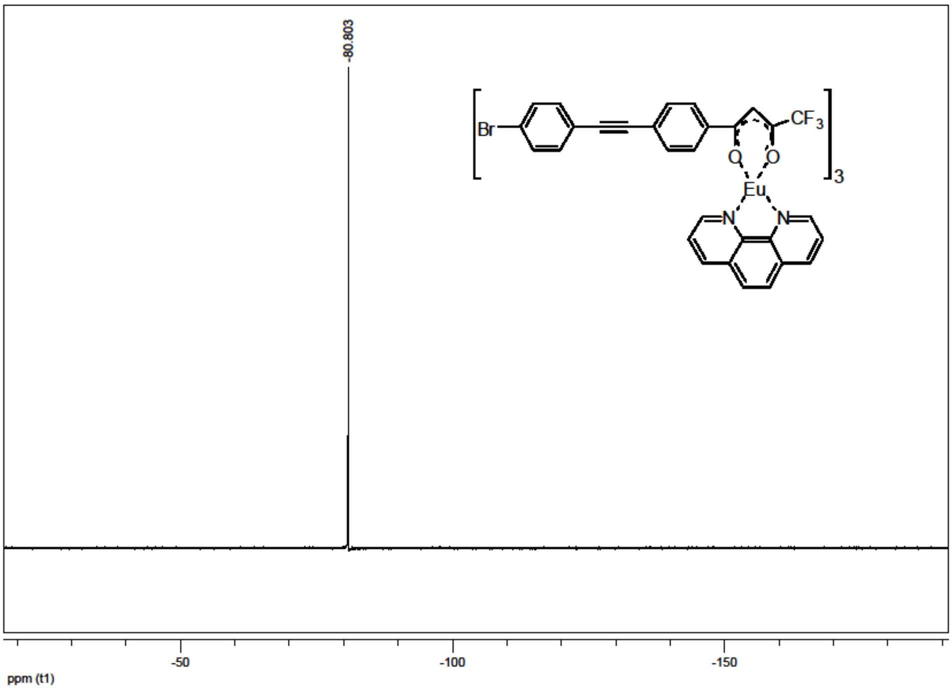

Figure S22. ^{19}F NMR spectrum of complex **3d** (282 MHz, $CDCl_3$).

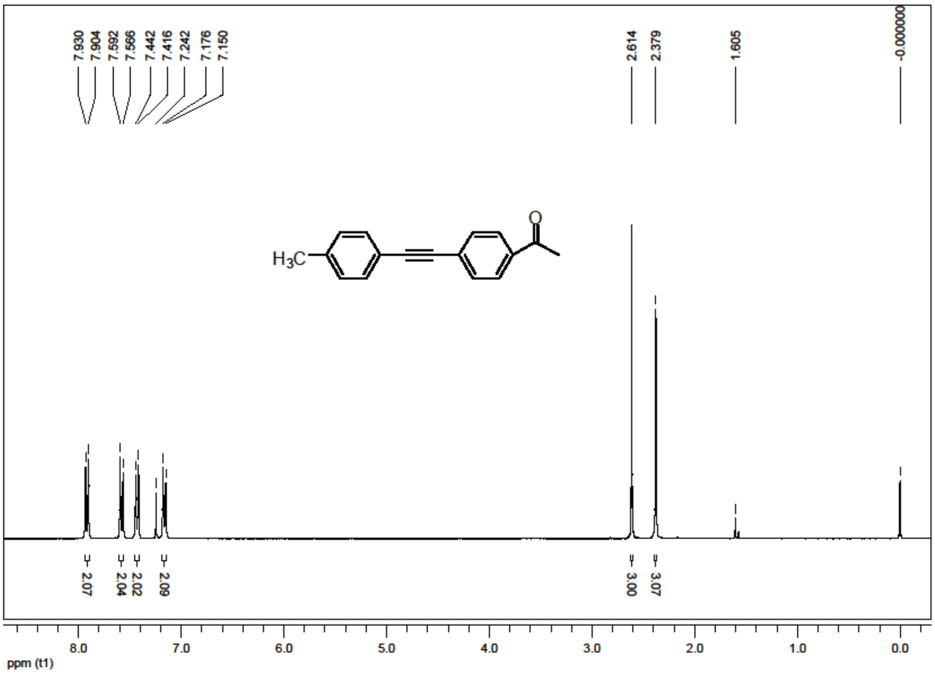

Figure S23. ^{1}H NMR spectrum of compound **1e** (300 MHz, $CDCl_3$).

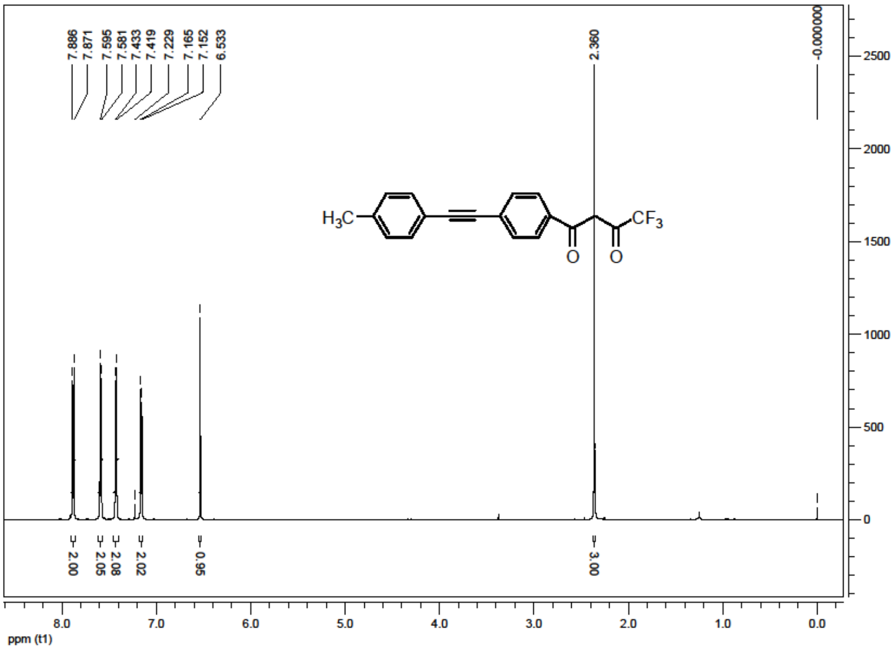

Figure S24. ^{1}H NMR spectrum of ligand **2e** (600 MHz, $CDCl_3$).

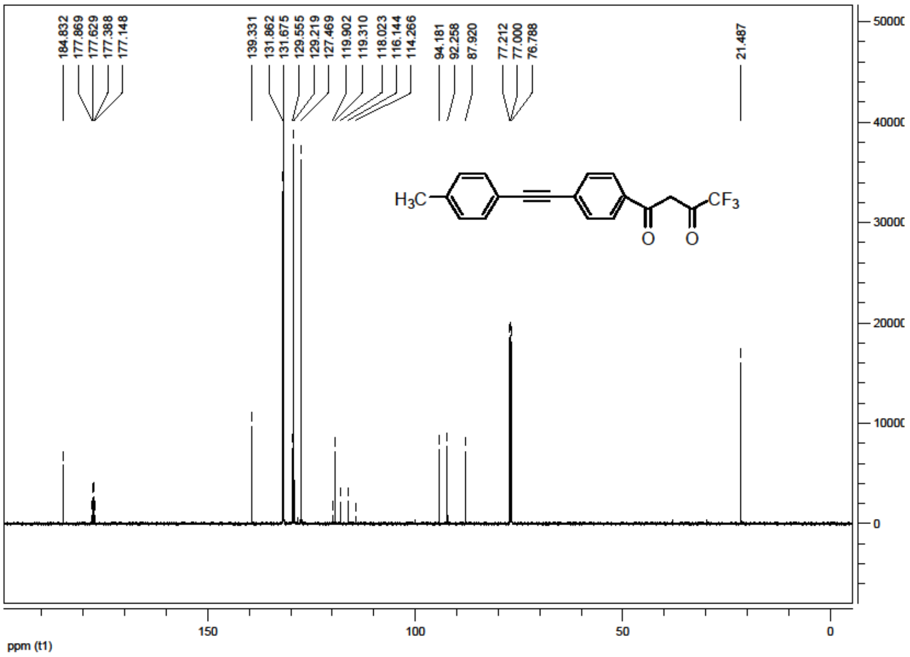

Figure S25. ^{13}C NMR spectrum of ligand **2e** (150 MHz, CDCl$_3$).

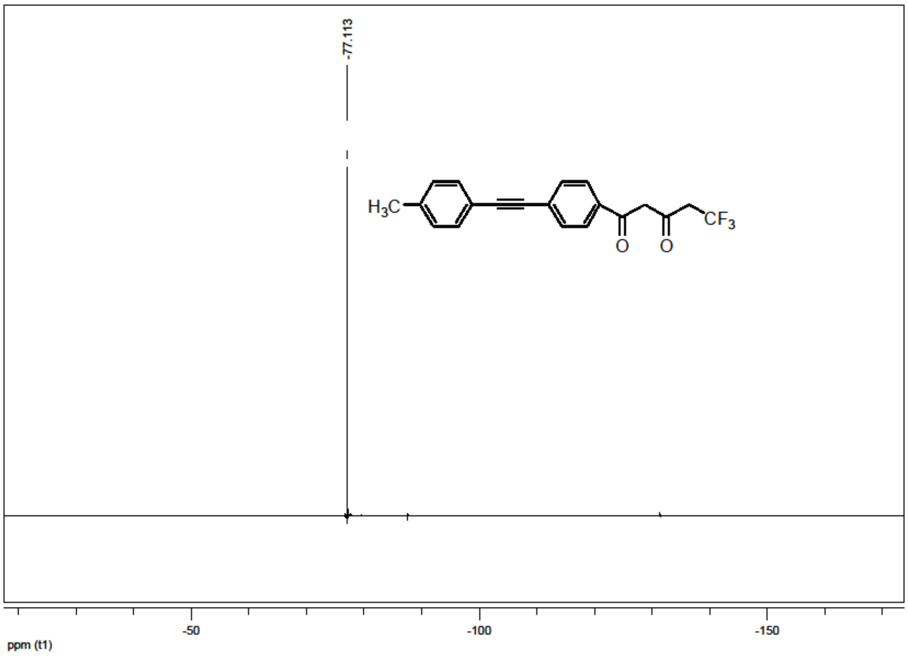

Figure S26. ^{19}F NMR spectrum of ligand **2e** (282 MHz, CDCl$_3$).

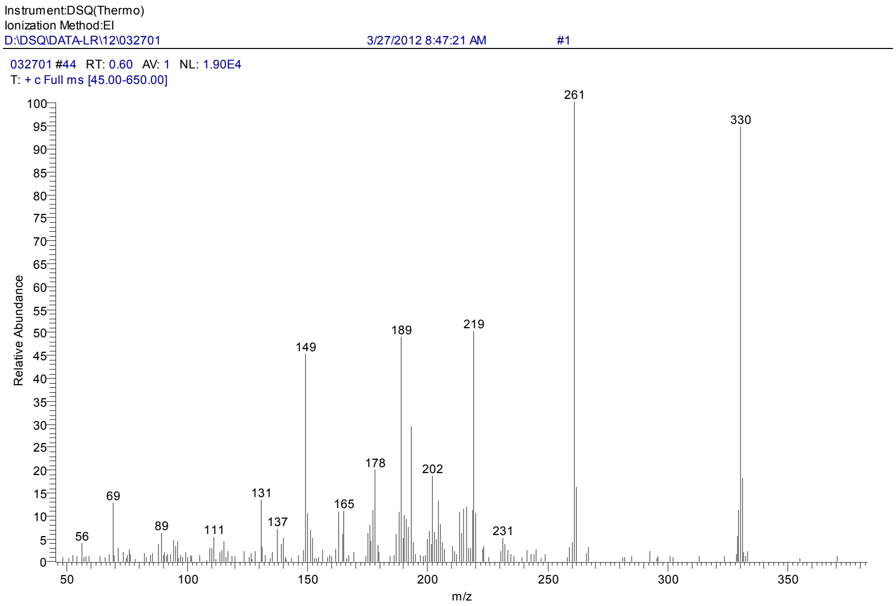

Figure S27. EI-MS spectrum of ligand **2e**.

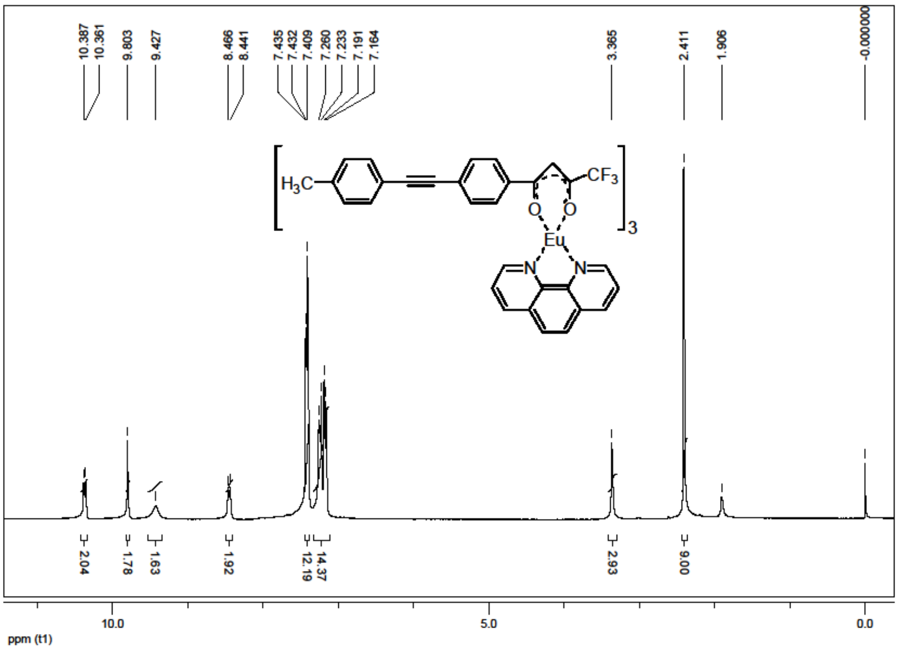

Figure S28. ^{1}H NMR spectrum of complex **3e** (300 MHz, $CDCl_3$).

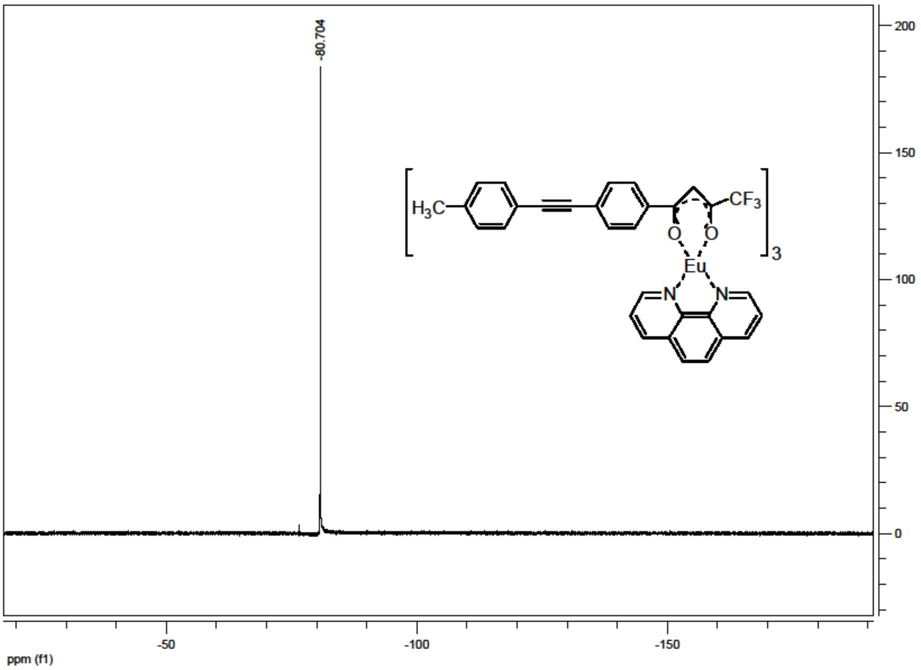

Figure S29. ^{19}F NMR spectrum of complex **3e** (282 MHz, $CDCl_3$).

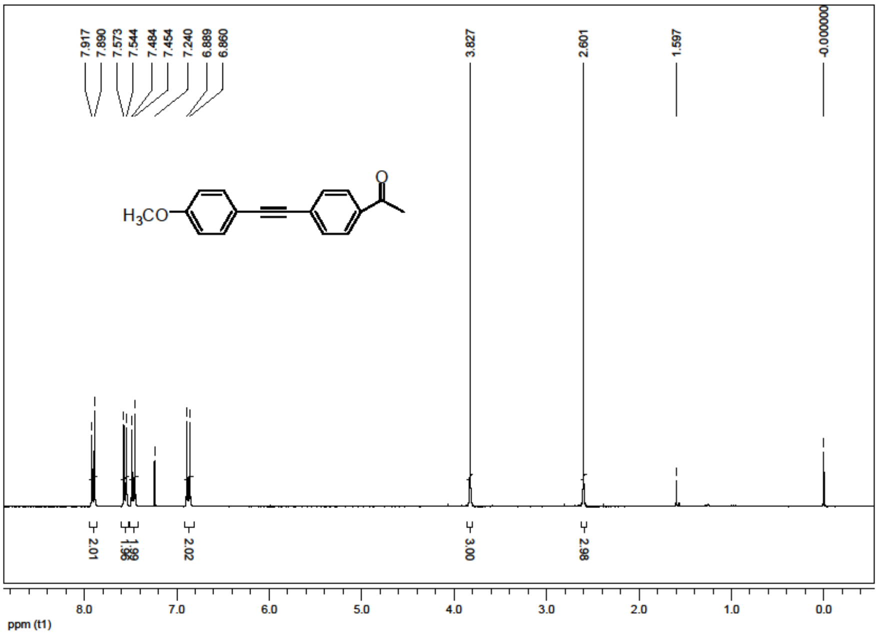

Figure S30. ^{1}H NMR spectrum of compound **1f** (300 MHz, $CDCl_3$).

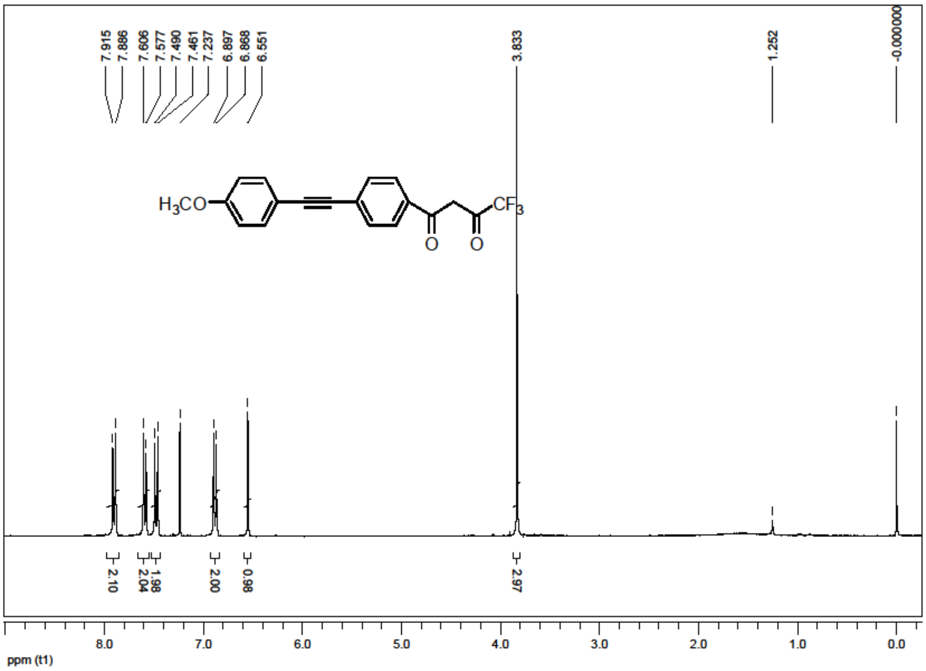

Figure S31. ^{1}H NMR spectrum of ligand **2f** (300 MHz, $CDCl_3$).

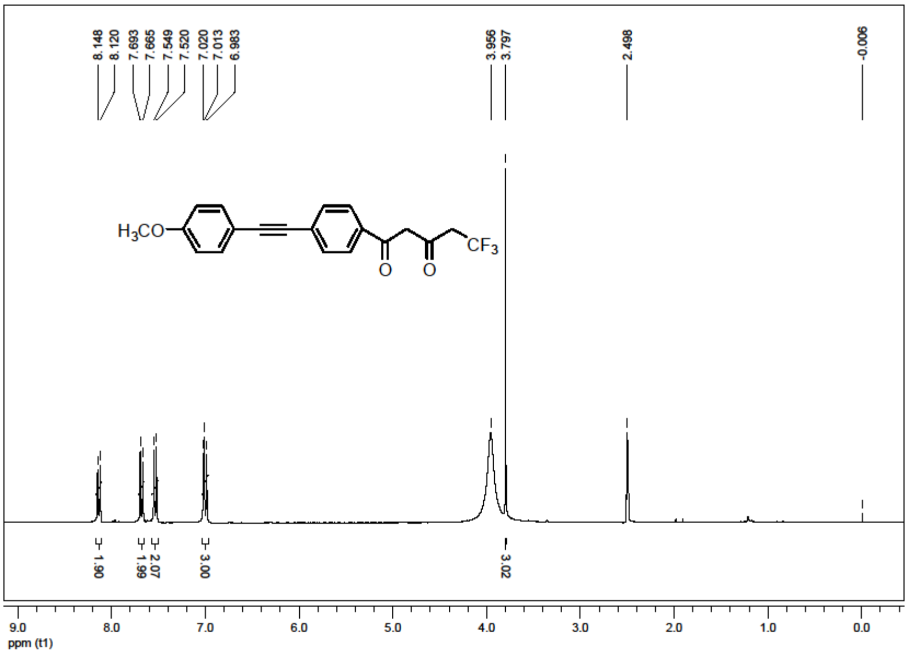

Figure S32. ^{1}H NMR spectrum of ligand **2f** (300 MHz, DMSO).

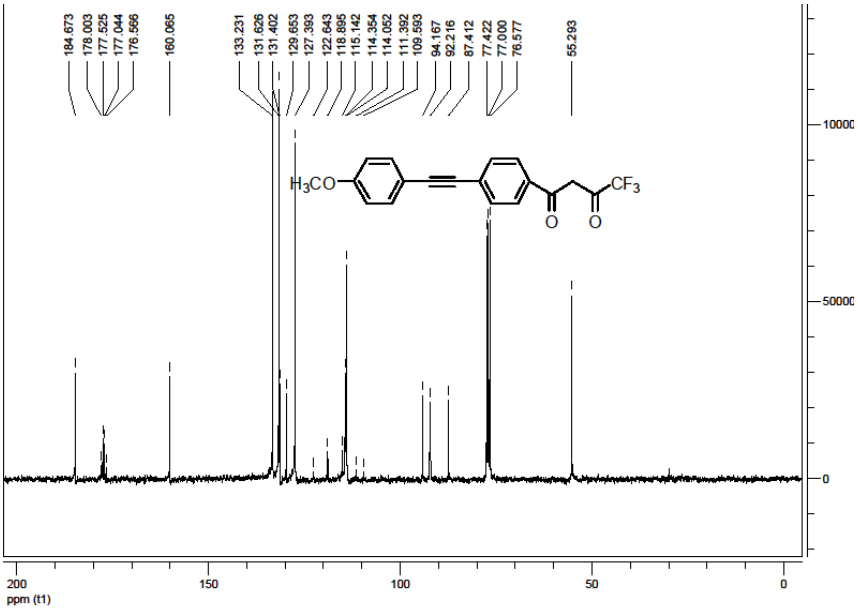

Figure S33. ^{13}C NMR spectrum of ligand **2f** (75 MHz, $CDCl_3$).

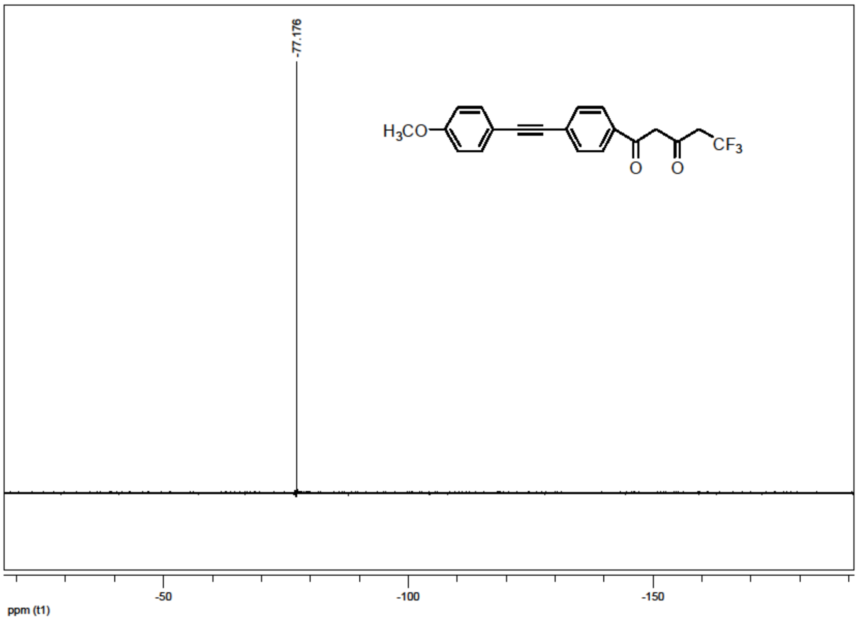

Figure S34. ^{19}F NMR spectrum of ligand **2f** (282 MHz, $CDCl_3$).

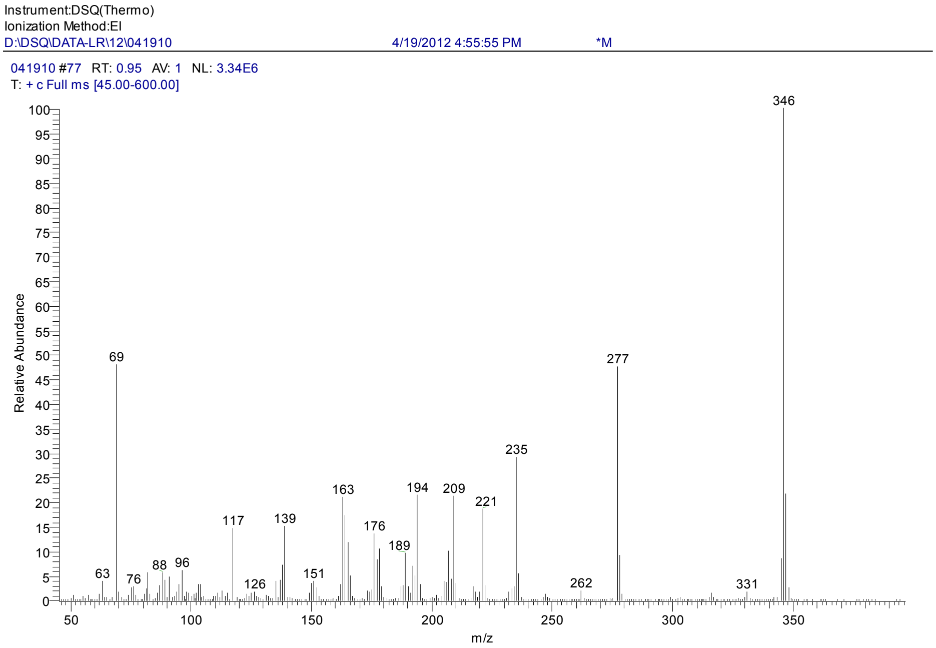

Figure S35. EI-MS spectrum of ligand **2f**.

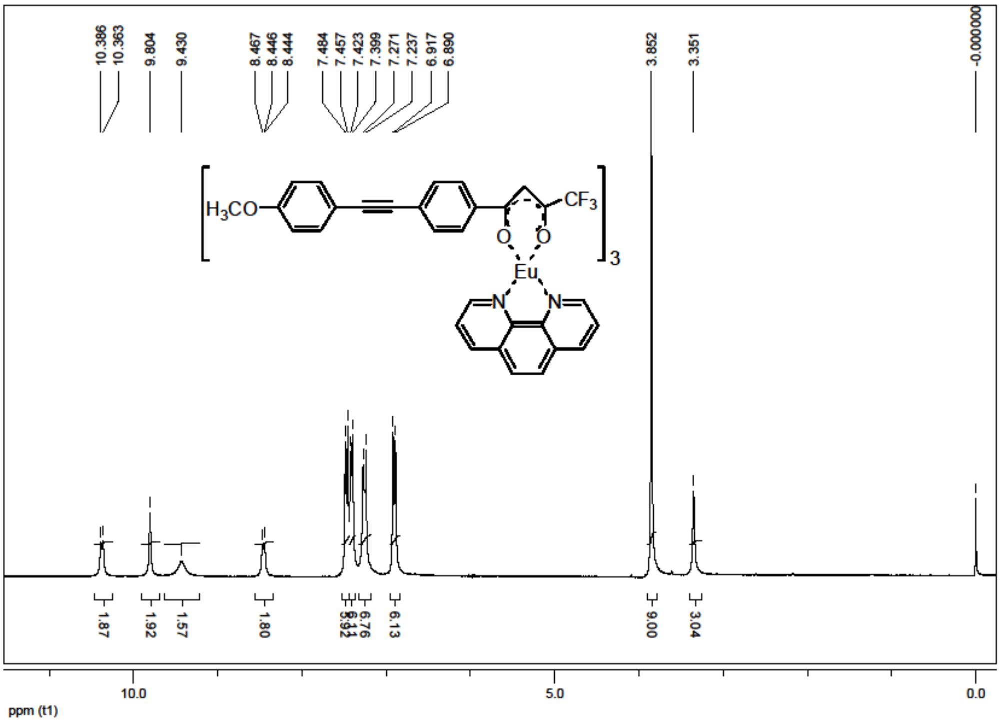

Figure S36. ^{1}H NMR spectrum of complex **3f** (282 MHz, $CDCl_3$).

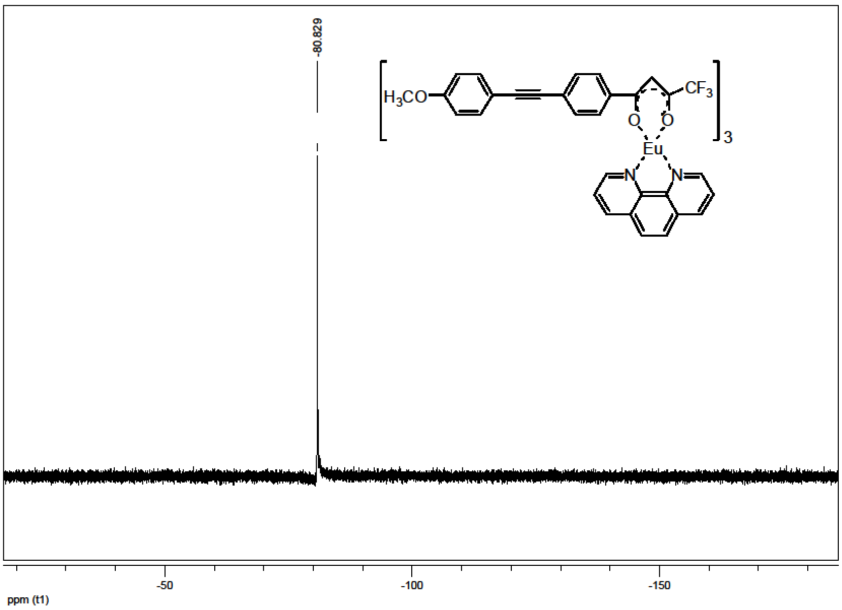

Figure S37. ^{19}F NMR spectrum of complex **3f** (282 MHz, $CDCl_3$).

4. TGA and DTG of complexes 3a–f

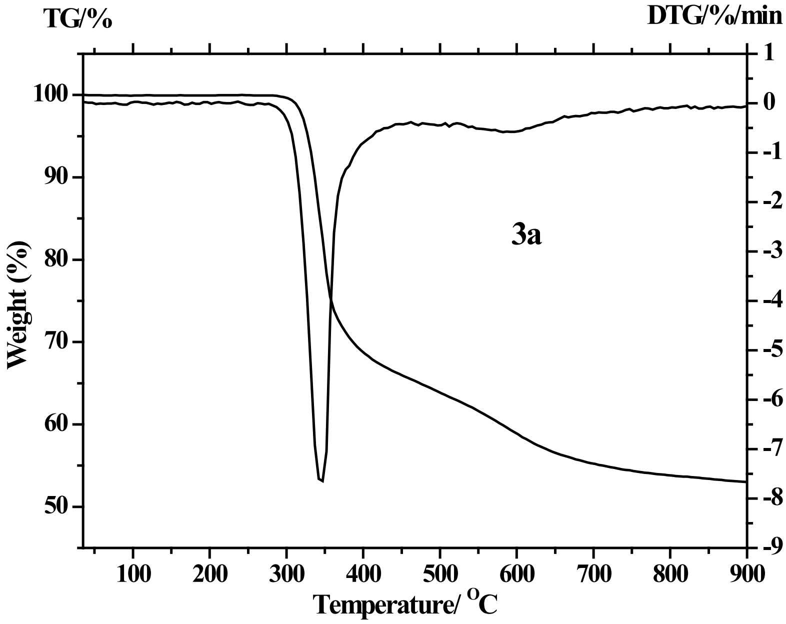

Figure S38. TGA and DTG of complex **3a**.

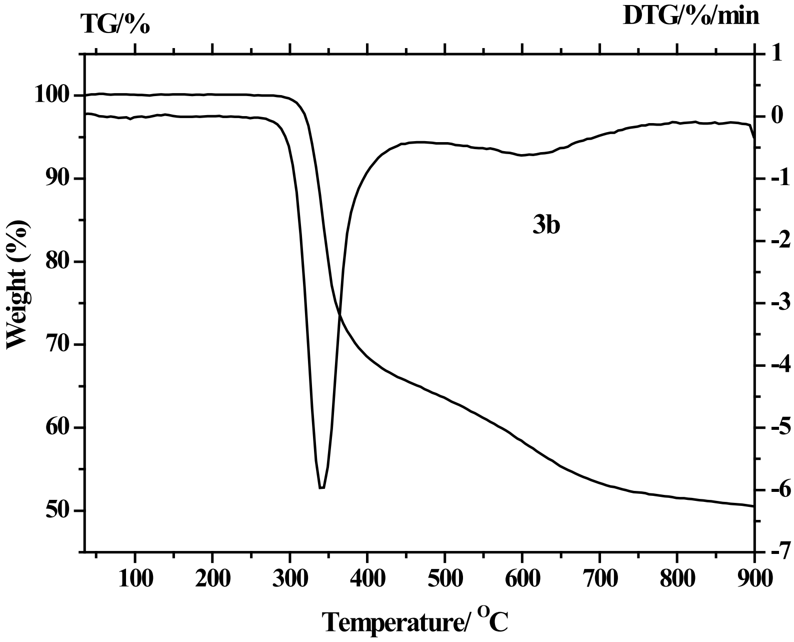

Figure S39. TGA and DTG of complex **3b**.

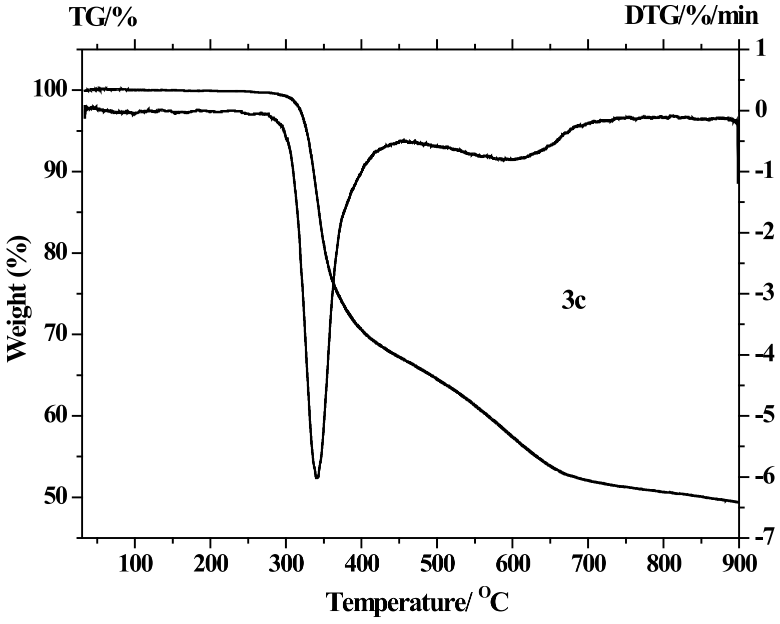

Figure S40. TGA and DTG of complex **3c**.

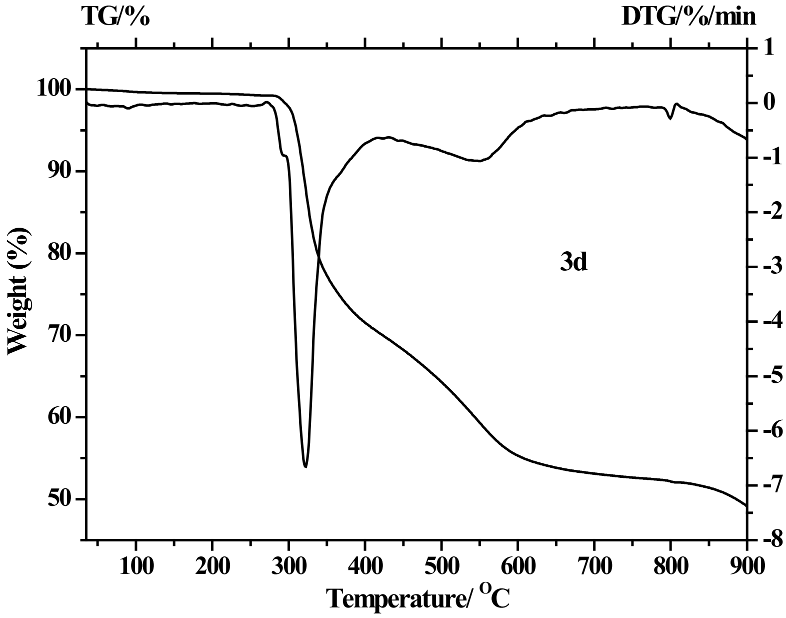

Figure S41. TGA and DTG of complex **3d**.

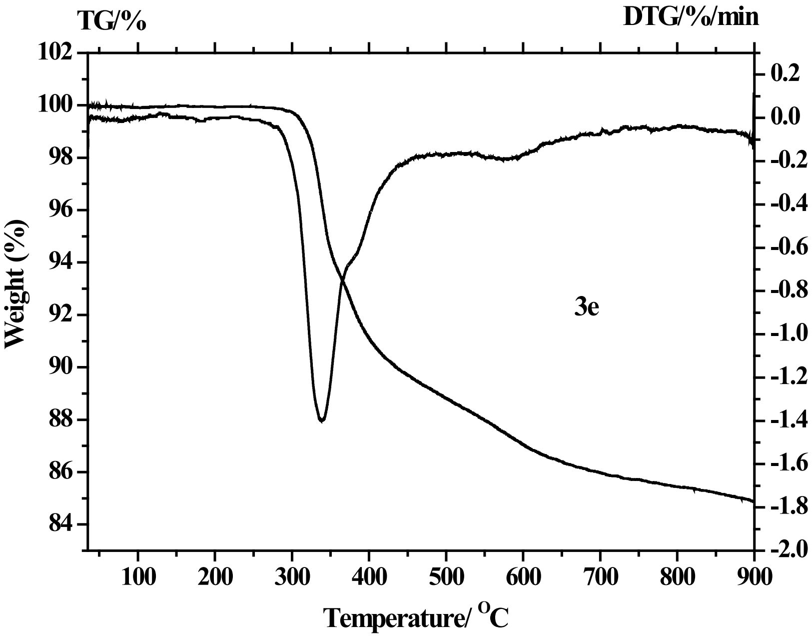

Figure S42. TGA and DTG of complex **3e**.

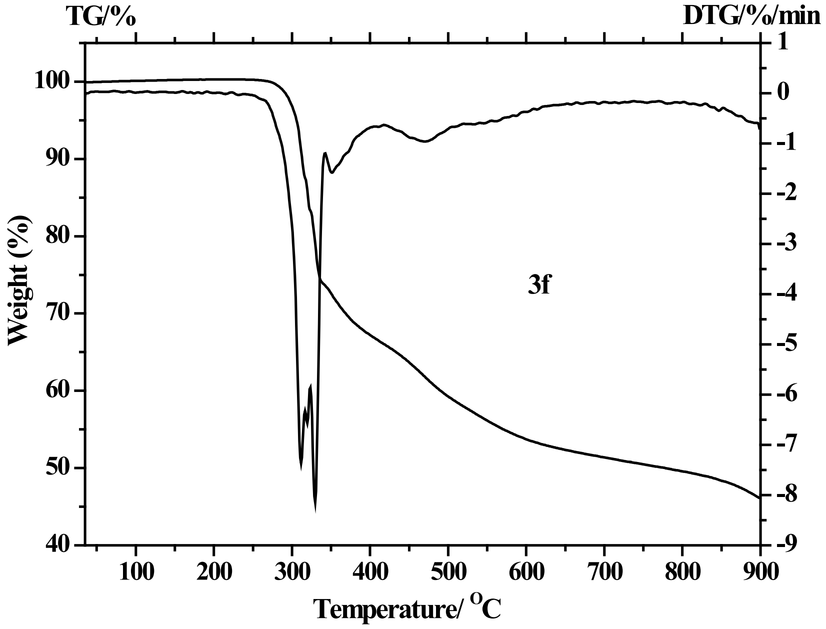

Figure S43. TGA and DTG of complex **3f**.

5. Magnified emission spectra of complexes 3a–f

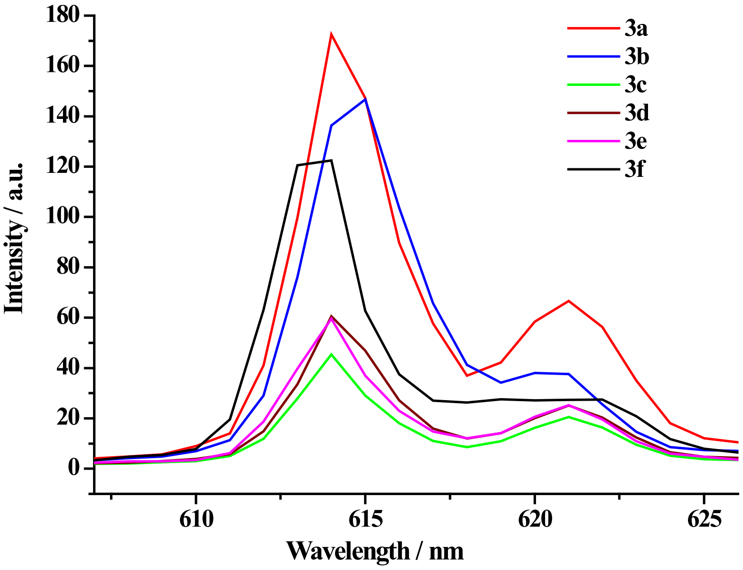

Figure S44. Magnified emission spectra of complexes **3a**–**f** in solid state (emission monitored at different λ_{ex}).

6. $^{5}D_0$ decay profiles of complexes 3a–f

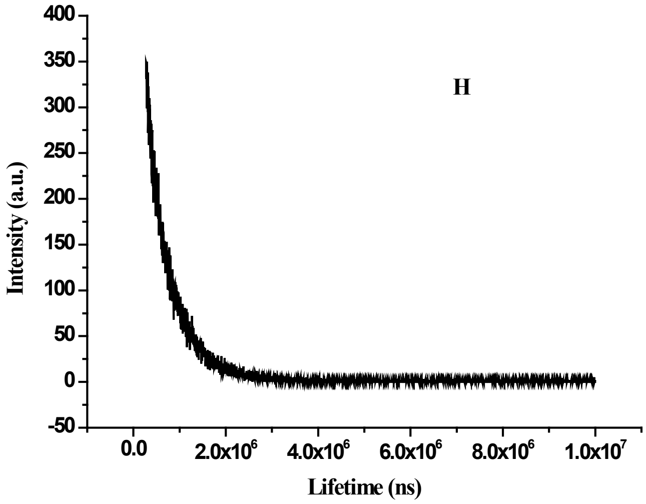

Figure S45. $^{5}D_0$ decay profile of complex **3a** (solid-state) excited at 398 nm and emission monitor around 614 nm.

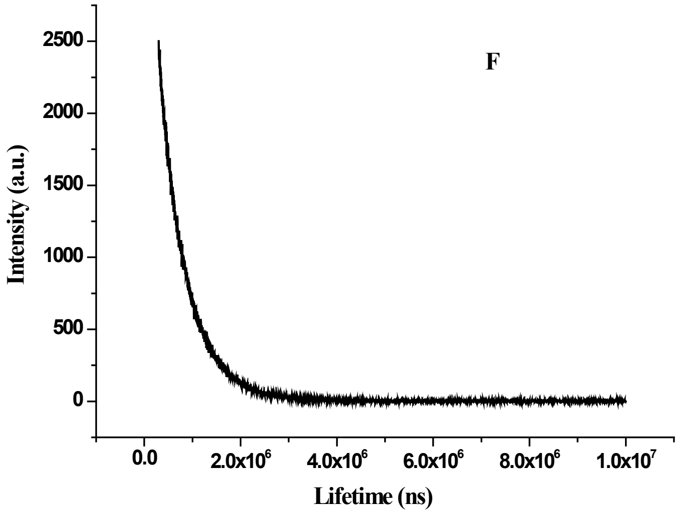

Figure S46. $^{5}D_0$ decay profile of complex **3b** (solid-state) excited at 397 nm and emission monitor around 614 nm.

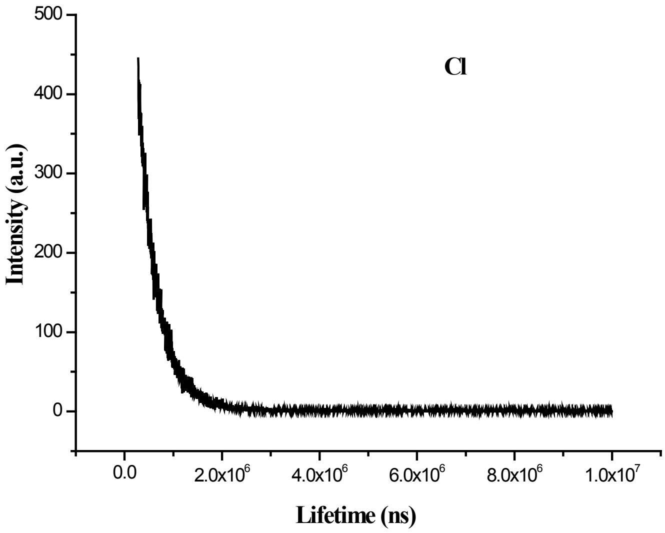

Figure S47. $^5D_0$ decay profile of complex **3c** (solid state) excited at 398 nm and emission monitored at 613 nm.

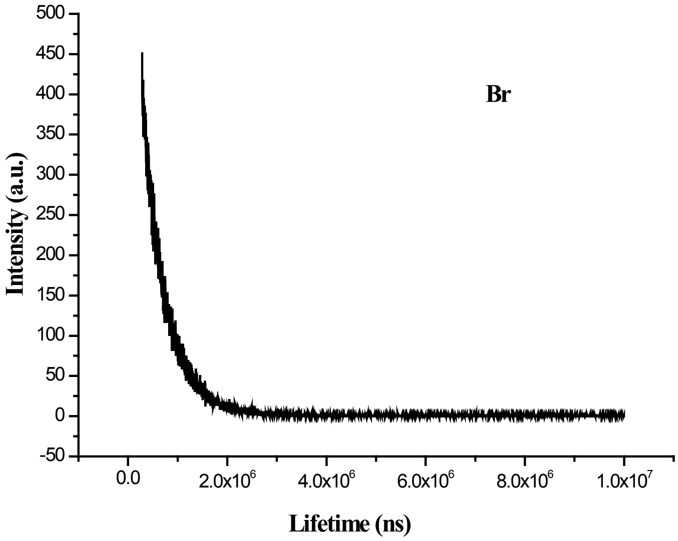

Figure S48. $^5D_0$ decay profile of complex **3d** (solid state) excited at 399 nm and emission monitored at 614 nm.

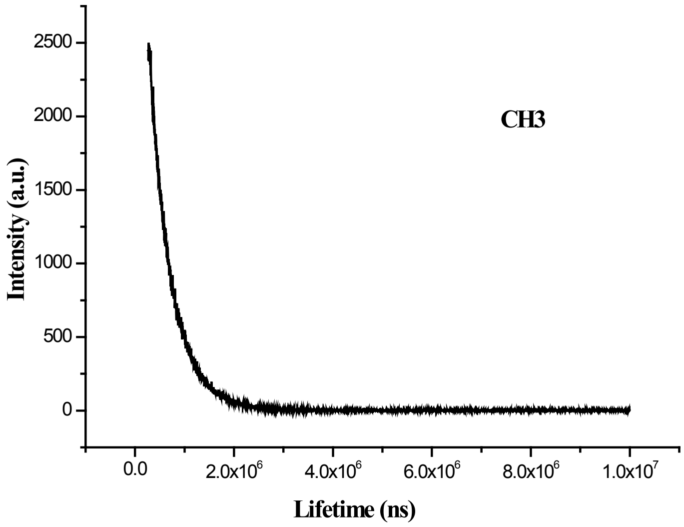

Figure S49. $^5D_0$ decay profile of complex **3e** (solid-state) excited at 389 nm and emission monitor around 614 nm.

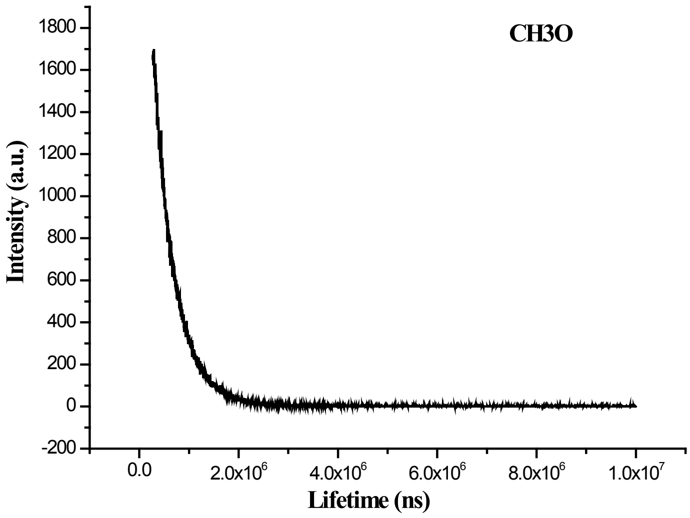

Figure S50. $^5D_0$ decay profile of complex **3f** (solid-state) excited at 425 nm and emission monitor around 614 nm.

7. Phosphorescence spectra of gadolinium(III) binary complexes

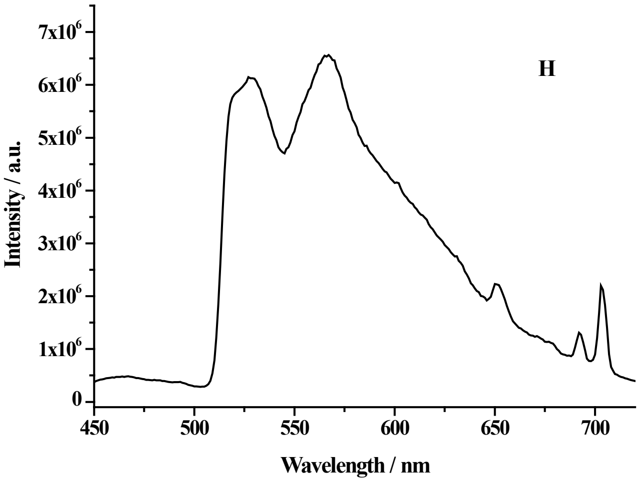

Figure S51. Phosphorescence spectrum of Gd(**2a**)$_3$·2H$_2$O (λ_{ex} = 330 nm, T = 77 K).

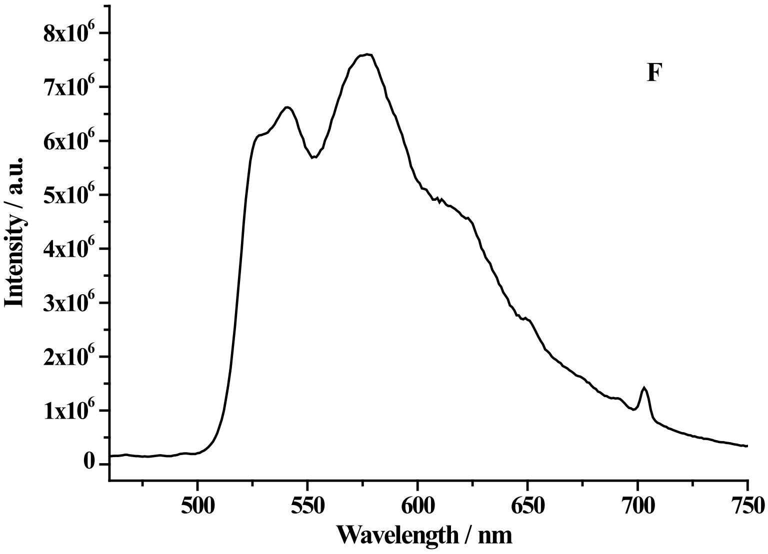

Figure S52. Phosphorescence spectrum of Gd(**2b**)$_3$·2H$_2$O (λ_{ex} = 329 nm, T = 77 K).

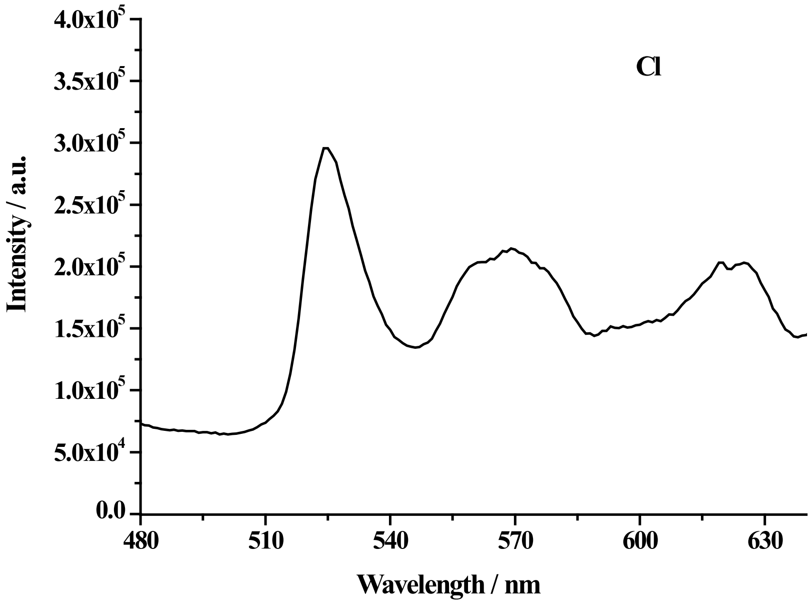

Figure S53. Phosphorescence spectrum of Gd(**2c**)$_3$·2H$_2$O (λ_{ex} = 330 nm, T = 77 K).

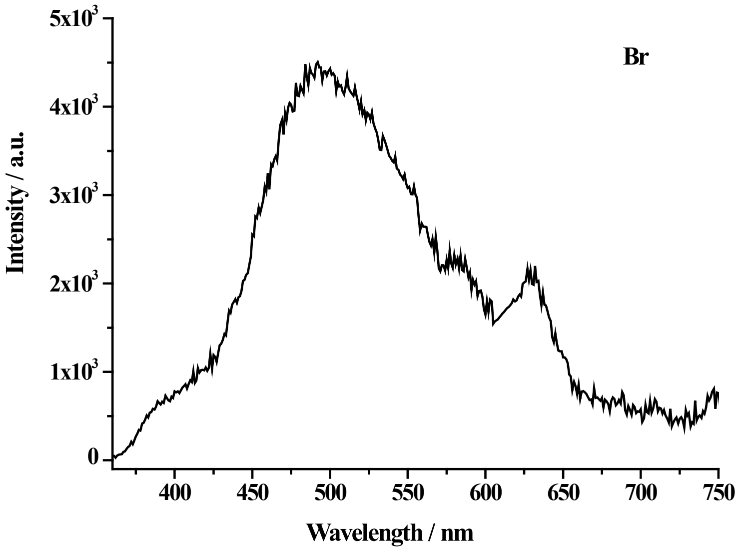

Figure S54. Phosphorescence spectrum of Gd(**2d**)$_3$·2H$_2$O (λ_{ex} = 331 nm, T = 77 K).

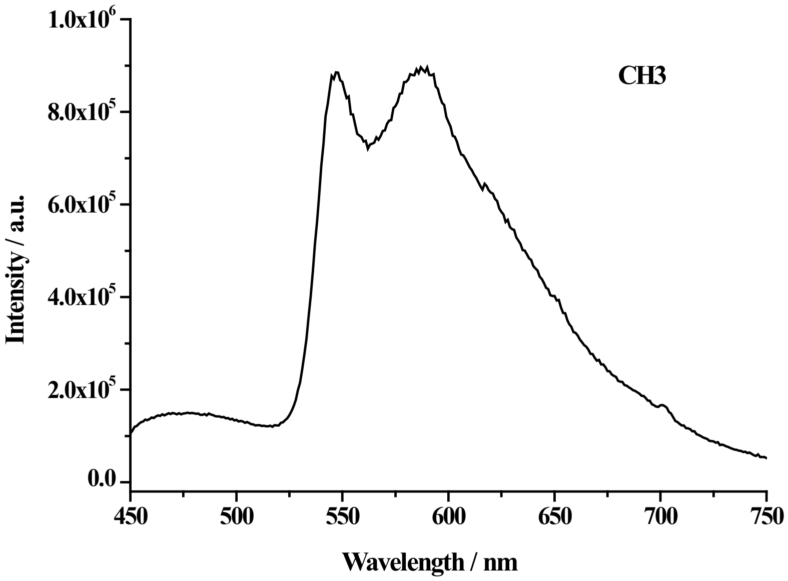

Figure S55. Phosphorescence spectrum of Gd(**2e**)$_3$·2H$_2$O (λ_{ex} = 333 nm, T = 77 K).

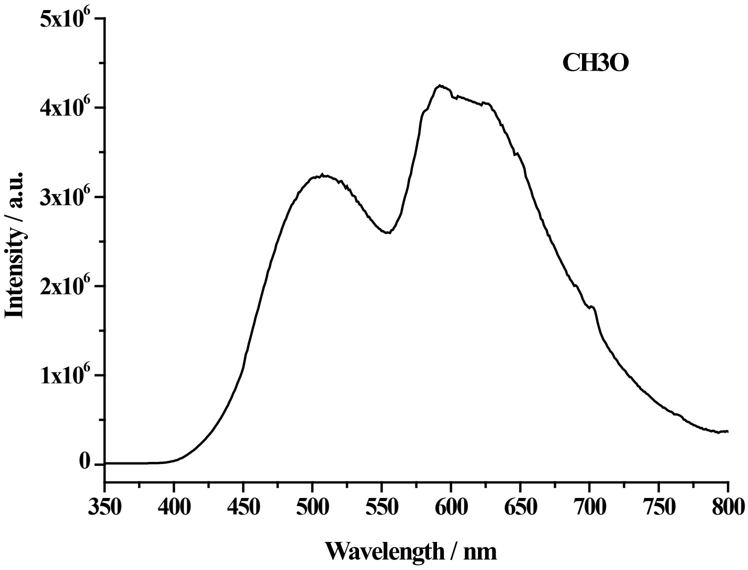

Figure S56. Phosphorescence spectrum of Gd(**2f**)$_3$·2H$_2$O (λ_{ex} = 338 nm, T = 77 K).

8. CV curves of ligands 2a–f

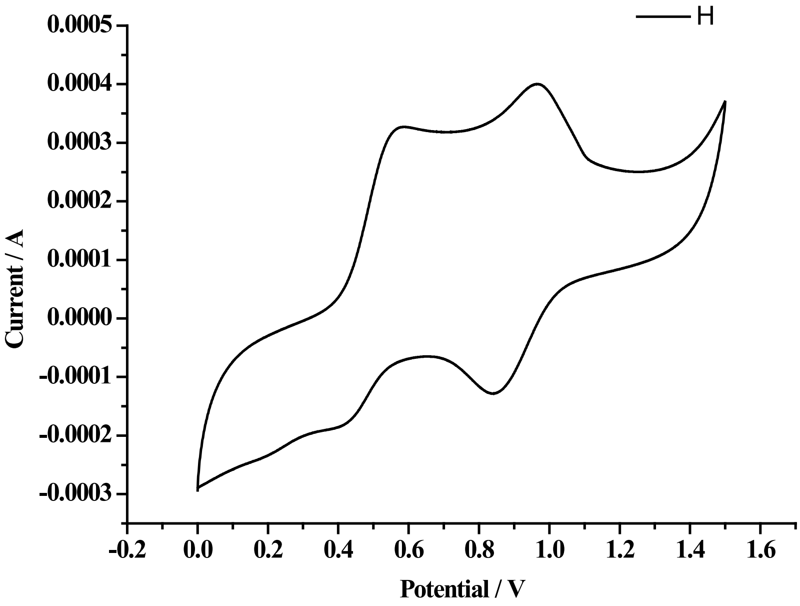

Figure S57. CV curve of ligand **2a** (7.5×10^{-5} mol/L) and ferrocene (Fc) (5.0×10^{-4} mol/L) in CH_2Cl_2.

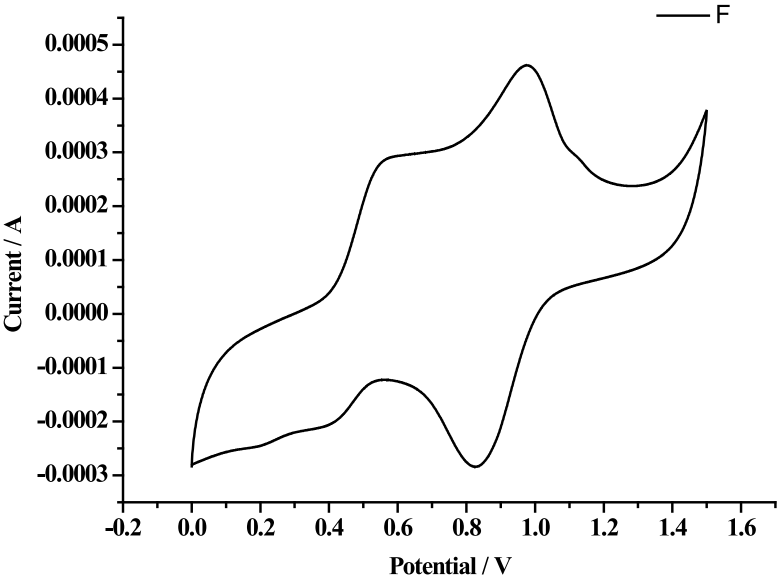

Figure S58. CV curve of ligand **2b** (7.5×10^{-5} mol/L) and ferrocene (Fc) (5.0×10^{-4} mol/L) in CH_2Cl_2.

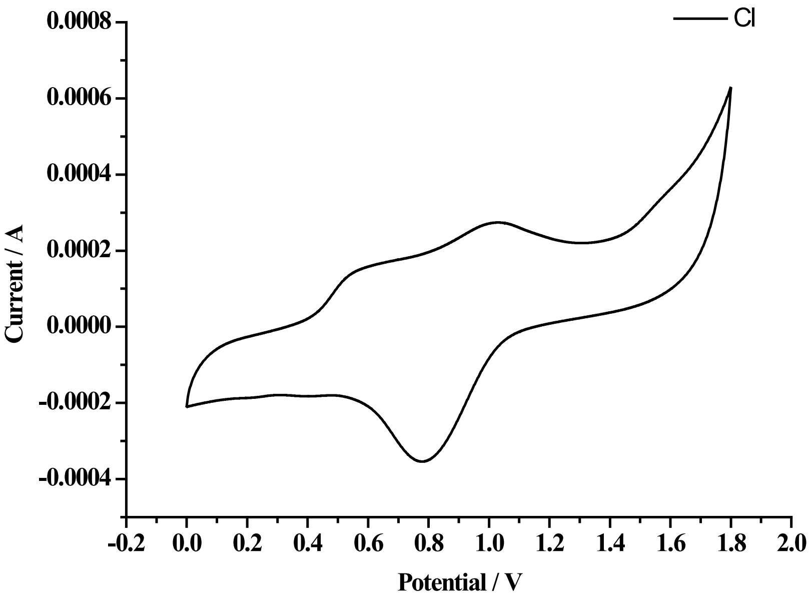

Figure S59. CV curve of ligand **2c** (7.5×10^{-5} mol/L) and ferrocene (Fc) (5.0×10^{-4} mol/L) in CH_2Cl_2.

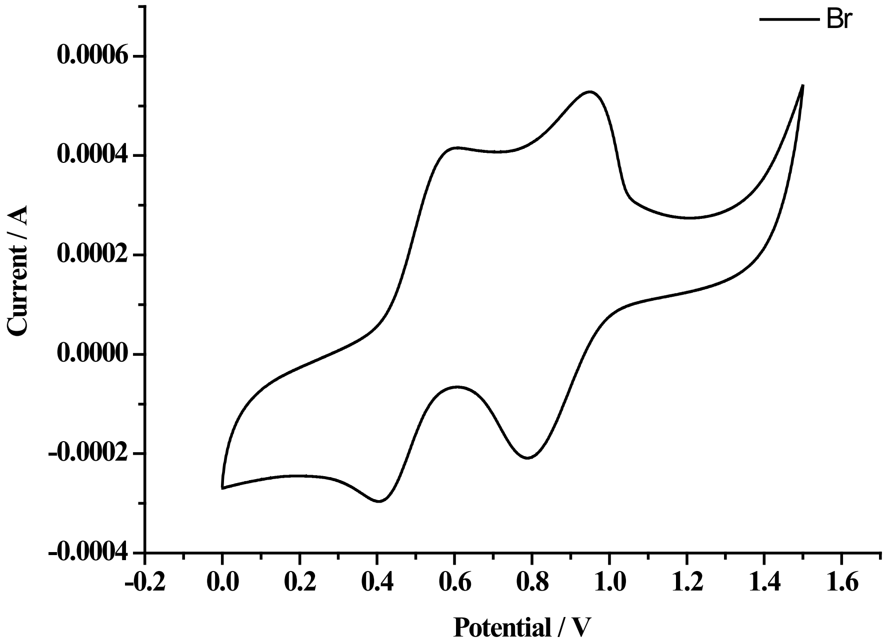

Figure S60. CV curve of ligand **2d** (7.5×10^{-5} mol/L) and ferrocene (Fc) (5.0×10^{-4} mol/L) in CH_2Cl_2.

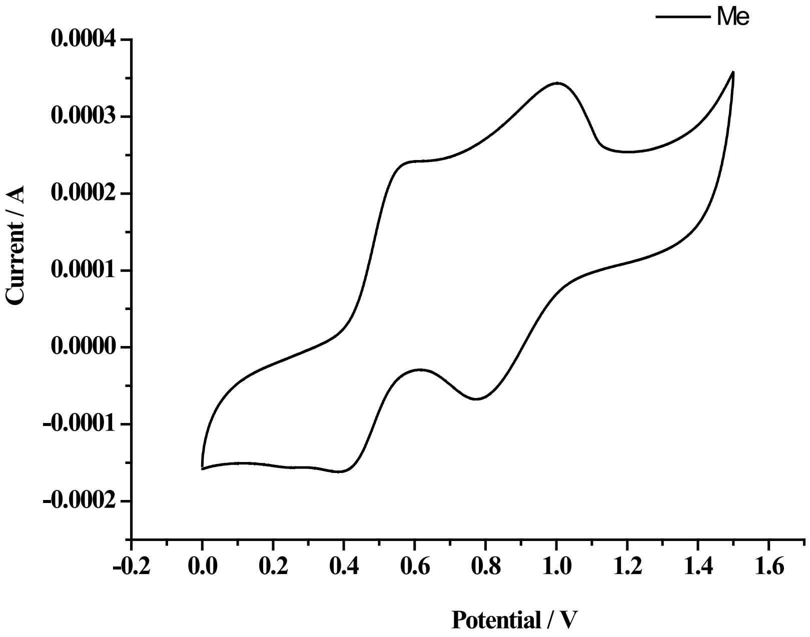

Figure S61. CV curve of ligand **2e** (7.5×10^{-5} mol/L) and ferrocene (Fc) (5.0×10^{-4} mol/L) in CH_2Cl_2.

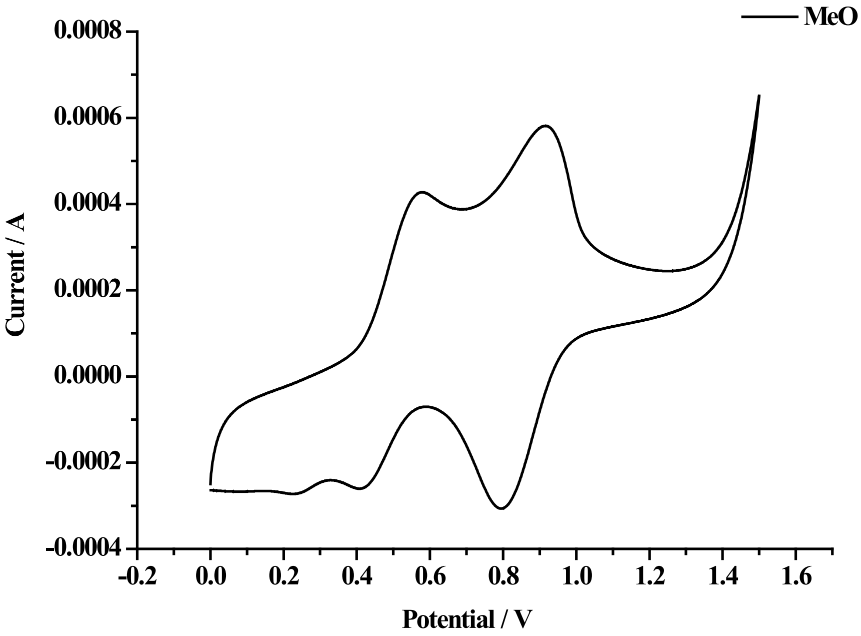

Figure S62. CV curve of ligand **2f** (7.5×10^{-5} mol/L) and ferrocene (Fc) (5.0×10^{-4} mol/L) in CH_2Cl_2.

9. Emission spectra and photographs of the fabricated LEDs

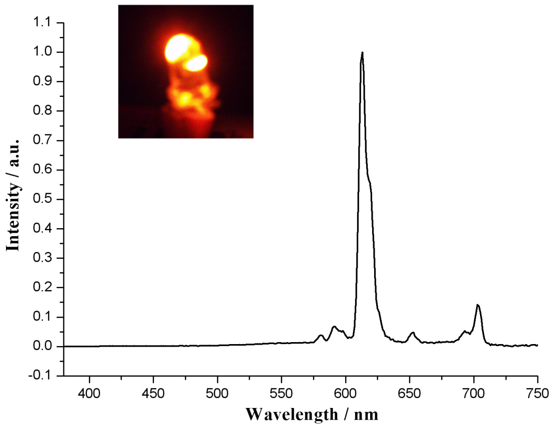

Figure S63. Emission spectrum of the near UV InGaN LED with complex **3a** under 20 mA forward bias (insert: a photograph of the LED in working state).

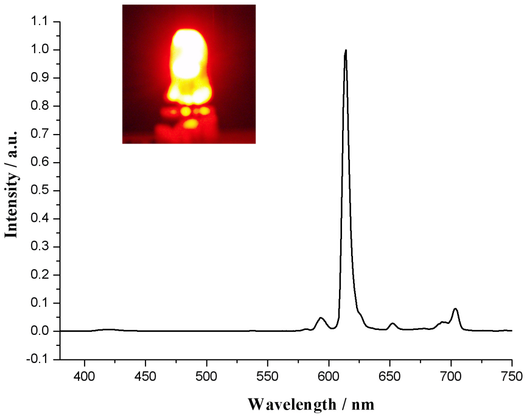

Figure S64. Emission spectrum of the near UV InGaN LED with complex **3b** under 20 mA forward bias (insert: a photograph of the LED in working state).

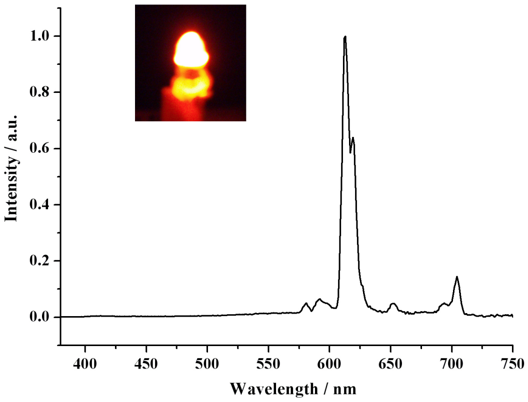

Figure S65. Emission spectrum of the near UV InGaN LED with complex **3c** under 20 mA forward bias (insert: a photograph of the LED in working state).

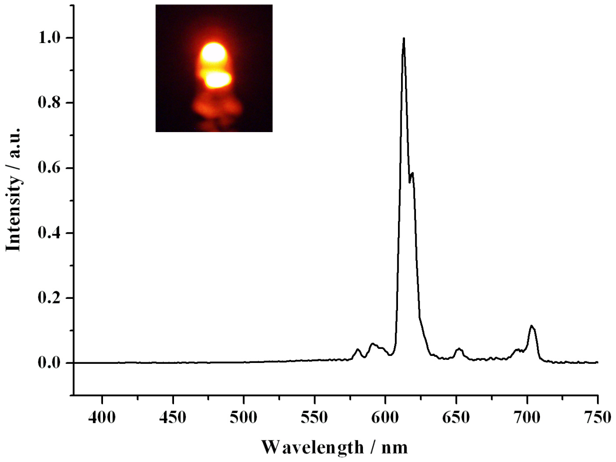

Figure S66. Emission spectrum of the near UV InGaN LED with complex **3d** under 20 mA forward bias (insert: a photograph of the LED in working state).

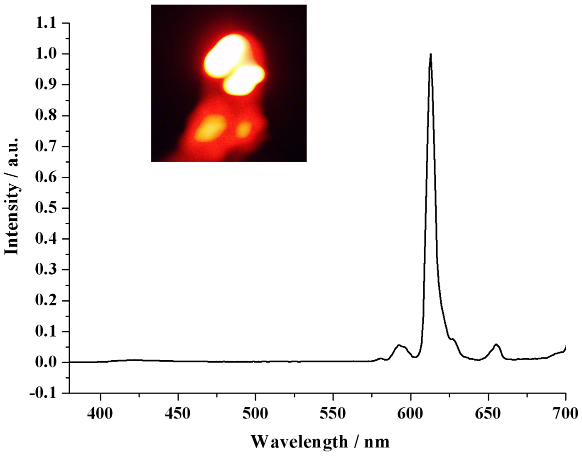

Figure S67. Emission spectrum of the near UV InGaN LED with complex **3e** under 20 mA forward bias (insert: a photograph of the LED in working state).

10. CIE chromaticity coordinates based on the emission spectra of the fabricated LEDs

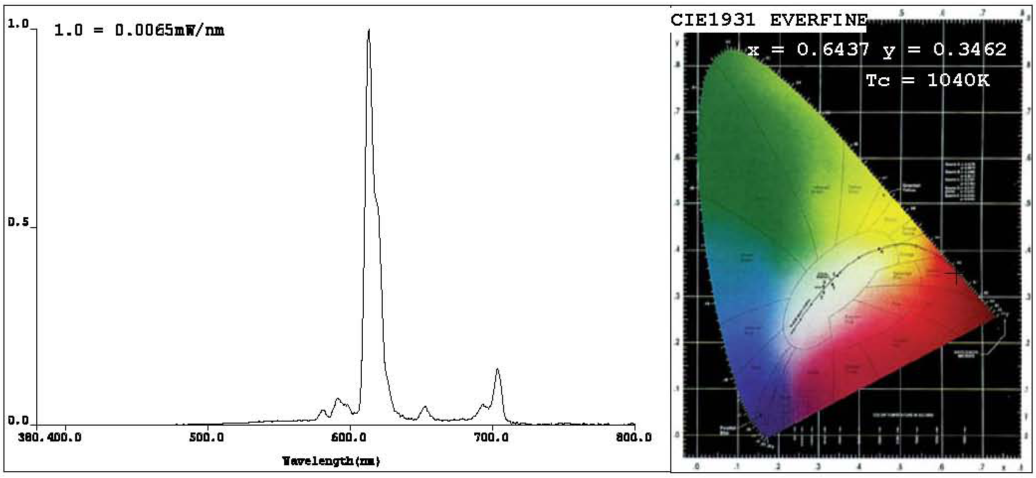

Figure S68. CIE chromaticity coordinates of the fabricated LED with complex **3a**.

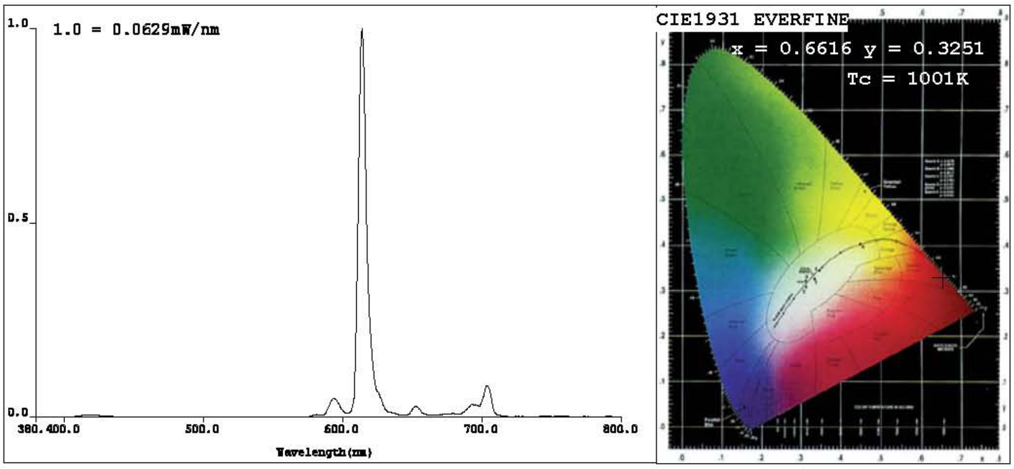

Figure S69. CIE chromaticity coordinates of the fabricated LED with complex **3b**.

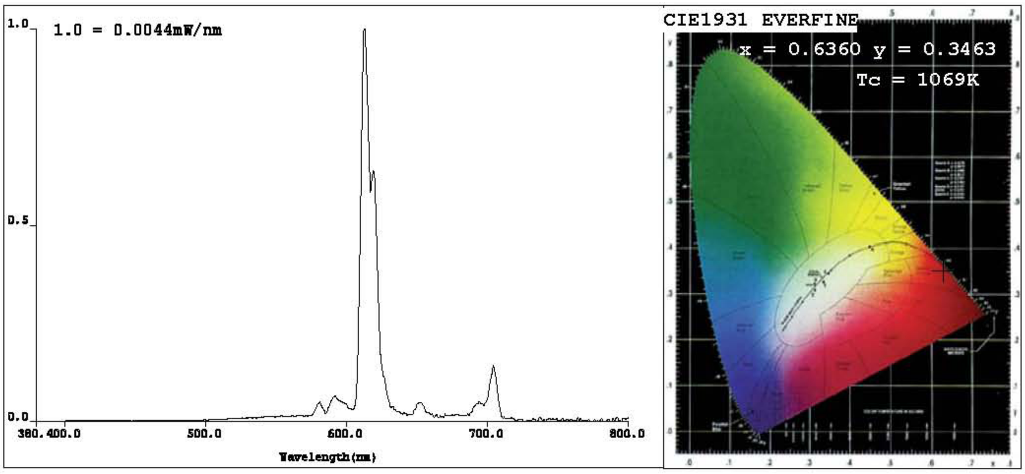

Figure S70. CIE chromaticity coordinates of the fabricated LED with complex **3c**.

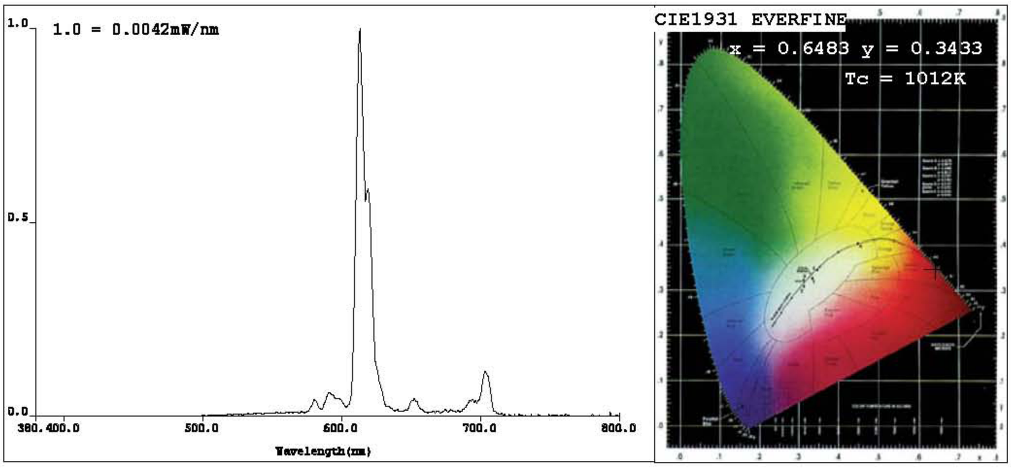

Figure S71. CIE chromaticity coordinates of the fabricated LED with complex **3d**.

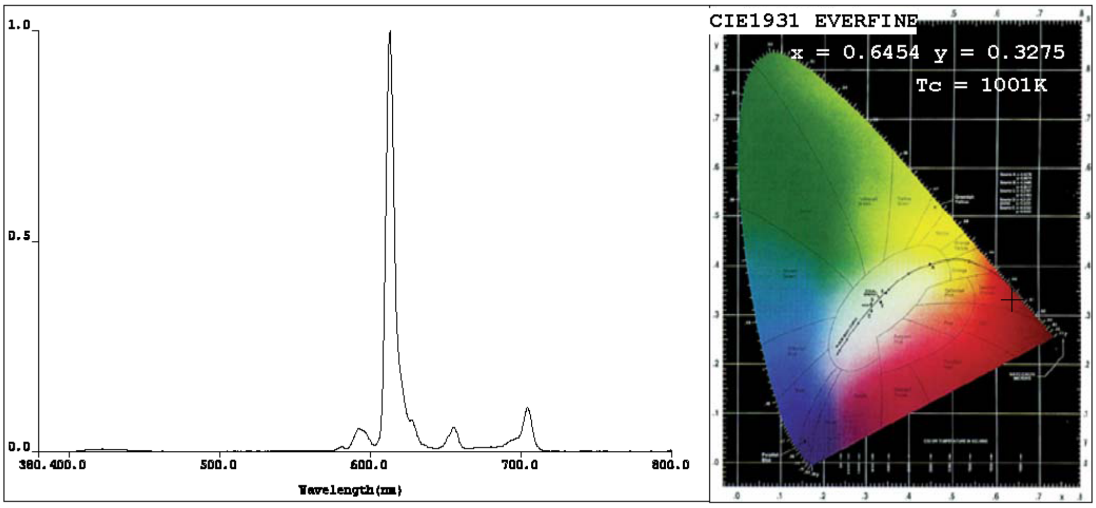

Figure S72. CIE chromaticity coordinates of the fabricated LED with complex **3e**.

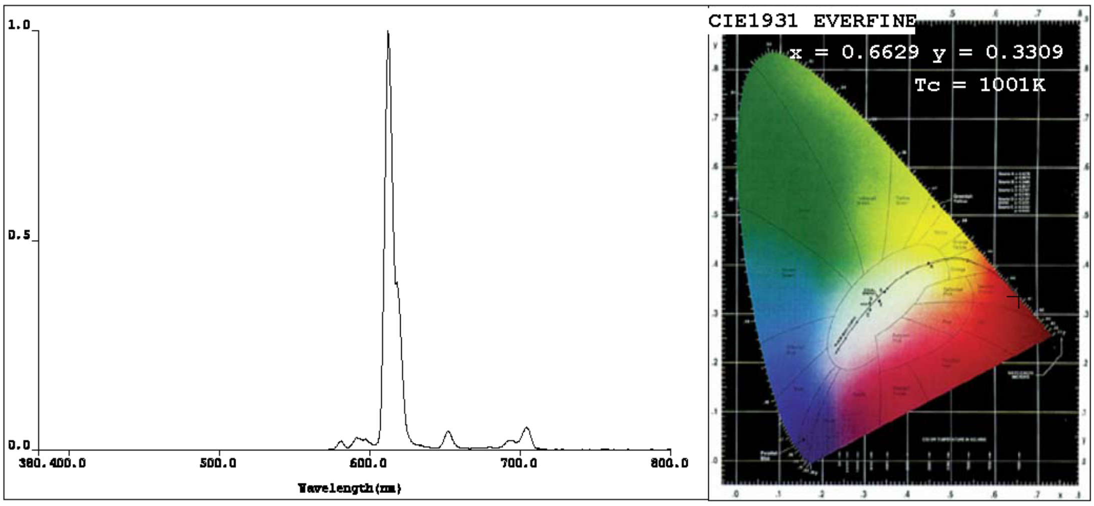

Figure S73. CIE chromaticity coordinates of the fabricated LED with complex **3f**.